Criticality in Brownian ensembles

Suchetana Sadhukhan and Pragya Shukla
Department of Physics, Indian Institute of Technology, Kharagpur 721302, India
(Received 28 October 2016; published 5 July 2017)

A Brownian ensemble appears as a nonequilibrium state of transition from one universality class of random matrix ensembles to another one. The parameter governing the transition is, in general, size-dependent, resulting in a rapid approach of the statistics, in infinite size limit, to one of the two universality classes. Our detailed analysis, however, reveals the appearance of a new scale-invariant spectral statistics, nonstationary along the spectrum, associated with multifractal eigenstates, and different from the two end-points if the transition parameter becomes size-independent. The number of such critical points during transition is governed by a competition between the average perturbation strength and the local spectral density. The results obtained here have applications to wide-ranging complex systems, e.g., those modeled by multiparametric Gaussian ensembles or column constrained ensembles.

DOI: 10.1103/PhysRevE.96.012109

I. INTRODUCTION

Recent studies of the localization to delocalization transitions, e.g., many body localization, Anderson localization, and random graphs, indicate a common mathematical structure underlying the statistical fluctuations of their linear operators [1–3]. The structure belongs to that of a Rosenzweig-Porter (RP) ensemble [4] or, equivalently, to a specific type of Brownian ensemble (BE), i.e., the one intermediate between Poisson and Gaussian ensembles [5]. This indicates a crucial but so far hidden statistical connection of the BEs with systems undergoing localization-delocalization transition. It is therefore natural to search for the criticality in BEs, which motivates the present study.

A Brownian ensemble, in general, refers to an intermediate state of perturbation of a stationary random matrix ensemble by another one of a different universality class [6–8]. The type of a BE, appearing during the cross-over, depends on the nature of the stationary ensembles and their different pairs may give rise to different BEs [8,9]. Similar nonstationary states may also arise in other matrix spaces, e.g., unitary matrix space, e.g., due to a perturbation of a stationary circular ensemble by another one [10–13]. BEs have been the focus of many studies in recent decades (for example, see Refs. [11,12,14] and the references therein) and a great deal of analytical and numerical information is already available about them. However, very few of these studies [1,5,15] probed the critical aspects of the BEs, which refers to a behavior different from the two stationary limits in infinite matrix size limit [16]. The search of criticality in BEs is important for several reasons. For example, the analytical study in Ref. [17] indicates that the statistical fluctuations of a wide range of complex systems are analogous to that of a Brownian ensemble, subjected to similar global-constraints, if their complexity parameters are equal irrespective of other system-details. (The complexity parameter is a function of the distribution parameters of the ensemble or alternatively a function of the average accuracy of the matrix elements, measured in units of the mean-level spacing.) A recent study [18] also reveals the connection of the BE to the random matrix ensembles with column or row constraints; the latter appear in diverse areas, e.g., bosonic Hamiltonians, such as phonons, and spin-waves in Heisenberg and XY ferromagnets, antiferromagnets, and spin-glasses, euclidean random matrices, random reactance networks, financial systems, and Internet-related Google matrix, etc. The knowledge of criticality in BEs can, therefore, be helpful in its search in other related ensembles.

The criteria for the critical statistics of energy levels and eigenfunctions was first introduced to an ensemble of disordered Hamiltonians undergoing localization-to-delocalization transition [19]. It has long been believed that a fractional value of the spectral compressibility and multifractal behavior of the eigenfunctions are signatures of the criticality in the ensemble [20,21]. In fact, these measures were used to claim the analogy of the Anderson ensemble (AE) at metal-insulator transition with that of the Power-law random-banded matrix (PRBM) ensemble [22]. The study in Refs. [5,23] indicates that the statistics of both of these ensembles can be mapped to that of the $\mathrm{BE}_{p\to o}$ (with subscript indicating the two end points, i.e., Poisson and Gaussian orthogonal ensemble); the BE is therefore expected to show similar critical features too. This is, however, at variance with the study in Ref. [1], which suggests the criticality in RP ensemble (and therefore in $\mathrm{BE}_{p\to o}$) is different from AE and PRBME; this suggestion is based on a perturbative analysis of the eigenfunction fluctuations and two point spectral correlation (also see Refs. [15,24–27] for related studies). The need for a clear answer motivates us to pursue an analytical calculation of the spectral compressibility and multifractality for the BEs. Although our approach is applicable for a generic BE of both Gaussian or Wishart type (i.e., intermediate between an arbitrary initial condition and the Gaussian or Wishart type stationary ensembles, these measures so far seem to be relevant in context of the ensembles undergoing localization to delocalization transition. To strengthen and support the theoretical analysis, we probe the behavior by numerical route, too, but that is confined to the Gaussian BEs between Poisson to GOE only.

The paper is organized as follows. Section II briefly introduces the Brownian ensembles in Hermitian matrix spaces. The diffusive dynamics for their eigenvalues and the eigenfunction components was analyzed in detail in Refs. [11,14,28], respectively. This information is used in Secs. III and IV to derive the parametric dependence of

the criticality measures, i.e., spectral compressibility, the multifractality spectrum, and eigenfunction correlations at two different energies. Here we also discuss the conditions under which they become critical. Although the results of Secs. III and IV are applicable for arbitrary initial conditions, the main interest in these measures arises, so far, from the quest to characterize the localization-to-delocalization transition. This motivates us to focus on the corresponding BE, i.e., $\mathrm{BE}_{p\to o}$ in subsequent sections and numerically verify our theoretical results for them. Section V briefly reviews the basic formulation for these BEs and presents the details of our numerical analysis. Section VI analyzes the reasons for the seemingly contradictory claims of the studies in Refs. [5] and [1]. We believe it can be explained on the basis of a rate of change of the local density of states, which affects the local statistical fluctuations. Section VII concludes with summary of our main results and open questions.

II. BROWNIAN ENSEMBLES: THE DEFINITION

Introduced by Dyson to model the statistical behavior of systems with partially broken symmetries and/or approximate conservation laws [6,7], a BE was originally based on the assumption of Brownian dynamics of matrix elements due to thermal noise. But currently a BE is also described as a single parameter governed diffusive state of the matrix elements of a randomly perturbed stationary ensemble [7–9,11]. Consider an ensemble of $N_a \times N$ rectangular matrices $A(\lambda) = \sqrt{f}(A_0 + \lambda V)$ with $f = (1+\lambda^2)^{-1}$ [11,14] and matrices A_0 and V distributed with probability densities $\rho_0(A_0)$ and $\rho_v(V)$. As clear, $A = A_0$ for $\lambda \to 0$, and $A \to V$ for $\lambda \to \infty$. The ensemble of rectangular matrices A can lead to three important classes of $N \times N$ Hermitian matrix ensembles: (i) Gaussian ensembles of matrices $H = A + A^\dagger$ with $N = N_a$, (ii) Wishart ensembles with matrices $L = A^\dagger A$ (also referred as Laguerre ensembles), and (iii) Jacobi ensembles of matrices S, which approach a form $S = (A^\dagger A + B^\dagger B)^{-1/2}\,(B^\dagger B - A^\dagger A)\,(A^\dagger A + B^\dagger B)^{-1/2}$. Our theoretical analysis in this paper is confined only to the first two ensembles.

A variation of strength λ of the random perturbation V leads to diffusion of the matrix elements $A_{kl} = \sqrt{f}(A_{0;kl} + \lambda V_{kl})$, which, by a suitable choice of $\rho_v(V)$, can be confined to a finite space. For example, for the Gaussian density of the V-ensemble, the Markovian character of the dynamics is preserved if considered in terms of a rescaled parameter Y given by the relation $f = e^{-2Y}$ [11]. For $\rho_v(V) = (\frac{1}{2\pi v^2})^{\beta N_a N/2} e^{-\frac{1}{2v^2}\,\mathrm{Tr}(VV^\dagger)}$, the diffusion equation for the matrix elements of X (with $X \equiv H$ or L) can explicitly be derived [11,14] (with $\beta = 1,2$ for X as real-symmetric or complex Hermitian, respectively). As discussed in Refs. [11,14,28], this in turn leads to the Y-governed diffusion equation for the joint probability distribution function (JPDF) of their N eigenvalues $e_k, k = 1 \to N$ and corresponding eigenfunctions. A direct integration of the JPDF diffusion equation over all eigenfunctions and $N - n$ eigenvalues leads to the diffusion equation for the nth order level-density correlation $R_n(e_1, e_2, \ldots, e_n)$. The measure $R_1(e)$ is also referred to as the ensemble average level density, with its fluctuations described by $R_n, n > 1$. As discussed in Ref. [8], the crossover in R_1 occur at a scale $Y \sim N\Delta_e^2$ with Δ_e as the local mean level spacing. The crossover in R_n is, however, rapid and occurs at scale $Y \sim \Delta_e^2$. For comparison of local spectral fluctuations around the level density, therefore, a rescaling of the eigenvalues by local mean level spacing $\Delta_e(e) = R_1^{-1}$ (also referred as unfolding) is necessary. This, however, leads to a rescaling of both R_n as well as the crossover parameter Y, with new parameter Λ_e given as

$$\Lambda_e(Y,e) = \frac{e^{\nu}\,(Y - Y_0)}{\Delta_e^2}, \tag{1}$$

with $\nu = 0,1$ for Gaussian and Wishart ensembles, respectively, and Y_0 is value of Y for initial ensemble $A = A_0$.

As discussed in Refs. [5,17], Λ_e also appears as the single parameter governing the spectral statistics of a multiparametric Gaussian ensemble (which includes Gaussian BEs as a special case); Y in this case is the function of all ensemble parameters, thus containing information about the ensemble complexity. Λ_e is, therefore, also referred to as the spectral complexity parameter.

It must be emphasized here that, before unfolding, the correlations in a BE depends on two parameters, namely, local mean level density and perturbation parameter Y. Although the unfolding maps the local mean level density to a constant, it, however, introduces a spectral-scale dependence in the rescaled evolution parameter Λ_e. The evolution of R_n for $n > 1$ is, therefore, different at different spectral scales, which implies the nonstationarity of local fluctuations of the BE. This is different from the stationary ensembles in which correlations R_n depends only on one parameter, i.e., local mean level density; the unfolding in this case results in a constant local level density and as a consequence, R_n become independent of spectral scale.

Contrary to spectral correlations, the local eigenfunction correlations in a BE are governed by different rescaling of Y sensitive to the measure under consideration [14,28]. This results in varying crossover speeds for the eigenfunction fluctuations and is in fact an indicator of the multiple scale dependence of the local eigenfunction intensity.

III. SIGNATURES OF CRITICALITY IN SPECTRAL STATISTICS

In general, the criticality in a JPDF of the eigenvalues can be defined as follows. A one-parameter scaling behavior of the distribution $P(\{e\})$ implies the existence of a universal distribution $P^*(\{e\}) = \lim_{N\to\infty} P(\{e\},\Lambda_e)$ if the limit $\Lambda^* = \lim_{N\to\infty} \Lambda_e(N)$ exists [16]. Thus, the size-dependence of Λ_e plays a crucial role in locating the critical point of statistics. If $|Y - Y_0| \propto N^\alpha$ and $\Delta_e \propto N^\eta$, then Eq. (1) gives $\Lambda_e \propto N^{\alpha-2\eta}$. A variation of size N in finite systems then leads to a smooth crossover of spectral statistics between an initial state ($\Lambda_e \to 0$) and the equilibrium ($\Lambda_e \to \infty$); the intermediate statistics belongs to an infinite family of ensembles, parameterized by Λ_e. However, for system-conditions leading to $\alpha = 2\eta$, the spectral statistics becomes universal for all sizes, Λ_e being N-independent; the corresponding system conditions can then be referred to as the critical conditions (or point). It should be stressed that the system conditions satisfying the critical criteria may not exist in all systems; the critical statistics, therefore, need not be a generic feature of all systems.

At critical value Λ^*, $R_n(r_1)$ (for $n > 1$) and, therefore, all spectral fluctuation measures are different from the two end points of the transition. i.e., $\Lambda_e = 0$ and ∞. Any of them can, therefore, be used, in principle, as a criteria for the critical statistics. A direct theoretical or numerical study of the JPDF of eigenvalues or the correlations R_n is, however, not the most suitable approach for the analysis. This has in the past led to introduction of many alternative measures [16], e.g., nearest-neighbor spacing distribution, number variance, spectral rigidity, etc. [7]. An important aspect of these measures is their spectral scale dependence. As mentioned in the previous section, the spectral correlations in BEs retain their energy-dependence through Λ_e even after unfolding and are nonstationary, i.e., vary along the spectrum [29]. Any criteria for the criticality in the spectral statistics can then be defined only locally, i.e., within the energy range, say δe_c, in which Λ_e is almost constant. From Eq. (1), $\frac{d\Lambda_e}{de} = 2(Y - Y_0)R_1\frac{dR_1}{de}$, which implies that δe_c is large only for regions where $R_1(e) \gg 2\frac{dR_1}{de}$.

The Λ_e-governed diffusion of the eigenvalues subjects the local spectral fluctuation measures also to undergo a similar dynamics. To determine their behavior at the critical point, it is necessary to first obtain the evolution equations for the relevant measures. The spectral compressibility being a popular measure as well as related to other criteria for spectral criticality, here we consider its evolution.

1. Spectral compressibility and its evolution

As mentioned in Sec. I, the spectral compressibility χ is an often used criteria for the criticality statistics in the ensembles of disordered Hamiltonians. A characteristic of the long-range correlations of levels, it is defined as, in a range r around energy e,

$$\chi(e,r) = 1 - \int_{-r}^{r} [1 - R_2(e,s)]\, ds, \tag{2}$$

where $R_2(e,r) \equiv R_2(e,e+r)$ is the two-point level density correlation at an energy e. As $R_2(e,r)$ is related to another two-point measure, namely, the number variance $\Sigma_2(e,r)$ (the variance in the number of levels in an interval of r mean number of levels), χ can also be expressed as the r rate of change of $\Sigma_2(e,r)$ [16,20,21]: $\Sigma_2(r) \sim \chi r$ for large r with $0 < \chi < 1$. (As the interest is often in large r behavior of χ at a fixed energy e, its dependence on energy e is usually suppressed.) In Ref. [20], χ was suggested to be related to the multifractality of eigenfunctions: $\chi = \frac{d-D_2}{2d}$ with D_2 as the fractal dimension and d as the system dimension. However, numerical studies indicated the result to be valid only in the weak-multifractality limit [30]. Later on, another criteria was introduced in terms of the level-repulsion (an indicator of short range correlation), measured by nearest-neighbor spacing distribution. The study in Ref. [19] showed that the nearest-neighbor spacing distribution $P(s)$ turns out to be a universal hybrid of the GOE at small s and Poisson at large s, with an exponentially decaying tail: $P(s) \sim e^{-\kappa s}$ for $s \gg 1$. Here κ is a constant and is believed to be related to χ: $\kappa = \frac{1}{2\chi}$.

For the spectrum of uncorrelated levels (no level repulsion), i.e., Poisson ensemble, $R_2(e,r) = 1$ which gives $\chi = 1$. But for a classical ensemble (e.g., Gaussian orthogonal or Unitary ensembles), the well-known sum rule $\int_{-N/2}^{N/2}[1 - R_2(e,r)]dr = 1$ gives $\lim_{r\to N/2} \chi(e,r) = 0$; this implies that a classical ensemble corresponds to the maximum level repulsion (i.e., zero compressibility) in the related symmetry class [7,9]. Clearly, if $\lim_{r\to N/2}\ \chi(e,r) \neq 0,1$, it characterizes a spectrum different from classical ensembles as well as uncorrelated spectrum. This characterization, however, is suitable only for the stationary spectrum (where unfolded spectral correlations are independent of the location along the energy axis). In case of the nonstationarity, the statistics varies along the energy-axis (even after unfolding) and one can at best define a local compressibility within an energy range $E_{\rm st}$ ($\ll$ total spectrum width) in which the local stationarity is valid. This led to the introduction of the following criteria for criticality: the spectral statistics is believed to be critical if

$$\lim_{r\to\infty}\ \lim_{N\to\infty}\ \chi(e,r) \neq 0, \neq 1. \tag{3}$$

(Note the order of limits on r and N are noninterchangeable. This leads to technical issues in numerical search for criticality in χ: the total number of levels N in the spectrum being finite, the maximum range of allowed r is $r \leqslant N_{\rm st} \ll N$, with $N_{\rm st} = \frac{E_{\rm st}}{\Delta_e}$, and it is not easy to realize a large r limit.)

To determine $\chi(e,r)$ from Eq. (2), a prior information of R_2 is needed. Unfortunately, an exact form of R_2 is known for very few BE cases, e.g., Poisson to GUE, GOE to GUE, uniform to GUE [8]. But the condition for a fractional value of χ can be obtained by general considerations. As discussed in Refs. [8,11], a variation of perturbation strength of the BE subjects $R_2(r)$ to undergo diffusion, described as

$$\frac{\partial R_2}{\partial \Lambda_e} = 2\frac{\partial}{\partial r}\left[\frac{\partial R_2}{\partial r} - \beta\frac{R_2}{r} - \beta\int_{-N/2}^{N/2}\frac{R_3(0,x,r)}{x}\,dx\right], \tag{4}$$

with $R_3(0,x,r)$ as the three-point level-density correlation and Λ_e given by Eq. (1). Note the above equation is applicable only locally, i.e., within spectral scale in which $R_1(e)$ is almost constant and R_2 is translationally invariant. The latter allows one to write $R_2(e,r) = R_2(r)$ but e-dependence enters through Λ_e. By differentiating Eq. (2) with respect to Λ_e, followed by a substitution of Eq. (4) and subsequent repeated partial integrations, leads to the following approximated closed-form equation for $\chi(r)$ (suppressing e-dependence of χ for clarity of presentation):

$$\frac{\partial\chi}{\partial\Lambda_e} = -4\left(\frac{\beta}{r} - \frac{\partial}{\partial r}\right)R_2(r;\Lambda_e) - 4\,\beta\int_{-N/2}^{N/2}\frac{R_3(0,x,r;\Lambda_e)}{x}\,dx. \tag{5}$$

An integration over Λ_e of the above equation now gives

$$\chi(r;\Lambda_e) = \chi(r;0) - \left[4\left(\frac{\beta}{r} - \frac{\partial}{\partial r}\right)\phi_1(r;\Lambda_e)\right] - 4\,\beta\,\phi_2(\Lambda_e), \tag{6}$$

where $\phi_1(r;\Lambda_e) = \int_0^{\Lambda_e} dt\ R_2(r,t)$, and $\phi_2(\Lambda_e) = \int_0^{\Lambda_e} dt \int_{-N/2}^{N/2} dx\ \frac{R_3(0,x;r,t)}{x}$. Further simplification of Eq. (6) is possible based on the following points:

(i) R_3 can also be expressed in terms of R_2: $R_3(0,x,r) = Y_3(0,x,r) + R_2(x) + R_2(r) + R_2(r-x) - 2$ with $Y_3(0,r,x)$ as the third-order cluster function [7,8]; (ii) the range of integral over x in the definition of ϕ_2 varies from $-N/2$ to $N/2$ and our interest is in the limit $N \to \infty$ followed by $r \to \infty$; (iii) as R_3 varies from $0 \to 1$, the main contribution to the integral over x in ϕ_2 comes from the neighborhood of $x = 0$. Thus, although the range of integration x varies from $-N/2$ to $N/2$, one needs to concern only with small x values, (iv) the cluster function $Y_3(0,r,x)$ vanishes if x or r or $|x-r|$ becomes large in comparison to the local mean level spacing [7]. In large r limit, therefore, one can approximate $R_2(r) \approx R_2(r-x) \to 1$, which leads to $\lim_{r\to\infty} R_3(0,x,r,t) \approx R_2(x,t)$. Using the latter, ϕ_2 can be expressed in terms of ϕ_1: $\phi_2(\Lambda_e) = \int_{-N/2}^{N/2} dx\ \frac{\phi_1(x,\Lambda_e)}{x}$. The lack of energy-level correlations at large r, i.e., $R_2(r,t) \to 1$ for arbitrary t, also gives

$$\lim_{r\to\infty, N\to\infty} \phi_1(r;\Lambda_e) = \int_0^{\Lambda^*} dt\ (\lim_{r\to\infty} R_2(r,t)) \approx \Lambda^*. \tag{7}$$

In the ordered limit $r \to \infty, N \to \infty$, Eq. (6) can now be reduced to the following form:

$$\begin{aligned}\lim_{r\to\infty} \chi(r;\Lambda^*) &= \lim_{r\to\infty, N\to\infty} \chi(r;\Lambda_e) \\ &= \lim_{r\to\infty, N\to\infty} \chi(r;0) - 4\,\beta\,\mathcal{I}_0, \end{aligned} \tag{8}$$

with $\Lambda^* = \lim_{N\to\infty} \Lambda_e$ and $\mathcal{I}_0 = \lim_{r\to\infty, N\to\infty} \phi_2(\Lambda_e) = \int_{-\infty}^{\infty} dx\ \frac{\phi_1(x,\Lambda^*)}{x}$. Further insight, however, can be gained by the following reasoning. As $\mathcal{I}_0 = \int_0^{\Lambda^*} dt \int_{-\infty}^{\infty} dr\ \frac{R_2(r,t)}{r}$, the dominant contribution to the integral over r comes from the region near $r = 0$. (This can also be seen as follows. In general, the eigenvalues at distances more than a system-specific spectral-range, say E_c around e, are uncorrelated. Here, E_c is a crucial spectral-range, hereafter, referred as the Thouless energy, as in the context of disordered systems in which case usually $E_c \sim \Delta_e$. This implies $R_2(r,t) \to 1$ for $r > N_e$, where $N_e = E_c/\Delta_e$, one can write $\int_{-\infty}^{\infty} dr\ \frac{R_2(r,t)}{r} = \int_{-\infty}^{-N_e} \frac{dr}{r} + \int_{N_e}^{\infty} \frac{dr}{r} + \int_{-N_e}^{N_e} dr\ \frac{R_2(r,t)}{r}$. Due to symmetry, the first two terms cancel out leaving only the last term.) Thus, $\mathcal{I}_0$ is sensitive to the short-range behavior of R_2, i.e., degree of level-repulsion in the spectrum.

It is worth noting here the advantage of Eq. (8) over Eq. (2): although calculation of χ by both Eqs. (2) and (8) depends on a prior knowledge of R_2 but later requires only its small-range behavior, which can easily be derived from Eq. (4), for arbitrary initial conditions, by neglecting the integral term. As an example, consider the BE intermediate to Poisson and Gaussian orthogonal ensemble (GOE); the small-r solution of Eq. (4) for this case can be given as $R_2(r,\Lambda) \approx (\frac{\pi}{8\Lambda})^{1/2}\, r\, e^{-r^2/16\Lambda}\, I_0(\frac{r^2}{16\Lambda})$, where I_0 is the modified Bessel function. Substitution of the latter in $\mathcal{I}_0$ leads to

$$\chi \approx 1 - 4\,\sqrt{2\pi}\,\eta_0\,\Lambda^*, \tag{9}$$

where $\eta_0 = \int_{-N_e}^{N_e} e^{-r^2}\, I_0(r^2)\, dr \approx \sqrt{\pi}$ with $\chi(r,0) = 1$ in Poisson limit.

Further insight in the large-r behavior of $\chi(r;\Lambda_e)$ can be derived through a Λ_e governed evolution equation in the spectral-region. The steps are as follows. Equation (2) gives $1 + \frac{1}{2}\frac{\partial\chi(r)}{\partial r} = R_2(r)$. In large-$r$ limit, this leads to the approximation

$$\begin{aligned}\int_{-\infty}^{\infty} \frac{R_3(0,x,r;\Lambda_e)}{x}\, dx &\approx \int_{-\infty}^{\infty} \frac{R_2(x,\Lambda_e)}{x}\, dx \\ &= \int_{-\infty}^{\infty} \frac{1}{2x}\frac{\partial\chi(x)}{\partial x}\, dx. \end{aligned} \tag{10}$$

Substitution of above relations in Eq. (5) gives Λ_e governed evolution of $\chi(r)$ for large r (with $\chi(\pm\infty)$ as constants):

$$\frac{\partial\chi}{\partial\Lambda_e} = \frac{-4\beta}{r} - \frac{2\beta}{r}\,\frac{\partial\chi}{\partial r} + 2\frac{\partial^2\chi}{\partial r^2} - 2\,\beta\,\int_{-\infty}^{\infty} \frac{\chi(x)}{x^2}\, dx. \tag{11}$$

As $0 < \chi(r;\Lambda_e) \leqslant 1$, the first and second term on the right side of the above equation can be neglected for large r and its integration over Λ_e gives $\lim_{r\to\infty} \chi(r;\Lambda_e) = \lim_{r\to\infty} \chi(r;0) - 2\,\beta\,\phi_3(\Lambda_e)$, with $\phi_3(\Lambda_e) = \int_0^{\Lambda_e} dt \int_{-\infty}^{\infty} dx\ \frac{\chi(x;t)}{x^2}$ (assuming $\frac{\partial^2\chi}{\partial r^2} \ll 1$ for large r). This reveals a bootstrapping tendency of $\chi(r)$, i.e., the dependence of χ at large r on its behavior near small r. Also note as both Λ_e and Λ^* are dependent on spectral scale e, χ is in general nonstationary along the spectrum.

IV. SIGNATURES OF CRITICALITY IN EIGENFUNCTION STATISTICS

The basis-variant nature of an ensemble, which is often the case at the critical point, implies a correlation between the eigenvalues and the eigenfunctions. The special features of the spectrum at the criticality are therefore expected to manifest in eigenfunctions too. For example, as indicated by many studies of the localization → delocalization transitions, the eigenfunctions within spectral range supporting critical statistics have multifractal structure. This has motivated three main criteria for the criticality in the eigenfunction fluctuations, namely, inverse participation ratio, multifractality spectrum, and eigenfunction correlations at different energy. Here we analyze these measures in context of the Brownian ensembles.

A. Inverse participation ratio and its evolution

The criticality in the wave functions is believed to manifest through large fluctuations of their amplitudes at all length scales and is often characterized by an infinite set of critical exponents related to the scaling of the moments of the wave-function intensity $|\Psi(r)|^2$ with system size [16,30]. The qth moment I_q of the wave-function intensity $|\Psi(r)|^2$, also known as qth inverse participation ratio, is defined as $I_q = \int dr |\Psi(r)|^{2q}$ (equivalently $I_q = \sum_n |\Psi_n|^{2q}$ in a N-dimensional basis with Ψ_n as the nth component of wave function Ψ). As revealed by the critical point studies of many disordered systems, an ensemble averaged I_q reveals an anomalous scaling with size N: $\langle I_q\rangle = N\,\langle|\,\Psi\,|^{2q}\rangle \sim N^{-\tau_q/d}$ with $\langle.\rangle$ implying an ensemble average with d as the system dimension; note $d = 1$ for a BE. Here, τ_q is a nondecreasing convex function with $\tau_0 = -d, \tau_1 = 0$.

The continuous set of exponents τ_q are related to the generalized fractal dimension D_q of the wave-function structure:

$\tau_q = (q-1)D_q$. At critical point, D_q is a nontrivial function of q, with $D_q = d$ and $D_q = 0$ for the eigenfunctions extended in a d-dimensional space and for completely localized ones, respectively. Further, τ_q is also related to anomalous dimension Δ_q, which distinguishes a multifractal state from an ergodic one and also determines the scale-dependence of the wave-function correlations: $\tau_q = d(q-1) + \Delta_q$ with $\Delta_0 = \Delta_1 = 0$ [30].

For spectral regions with almost constant level density, the parametric-evolution of the average inverse participation ratio for a generic BE of Gaussian or Wishart type can be given as [14,28]

$$\overline{\langle I_q(\Lambda_I)\rangle} = e^{-t_2\,\Lambda_I}\left[\overline{\langle I_q(0)\rangle} + t_1\int_0^{\Lambda_I}\overline{\langle I_{q-1}(r)\rangle}\; e^{t_2\,r}\,dr\right], \tag{12}$$

with symbol $\overline{x}$ implying a local spectral averaging of a variable x. Here, $t_1(q) = \frac{2(q-1)+\beta}{\beta}\langle|\Psi(r)|^2\rangle_e$, $t_2(q) = 1 + \frac{1}{q\,\mathcal{K}_2}[(\frac{2}{\beta})^\nu + \frac{2\nu N}{E_c}]$ and $\Lambda_I = q\;\beta\;\mathcal{K}_2\;(Y - Y_0)$, $\mathcal{K}_s \approx \frac{2^s\,N}{E_c^s}\;e^\nu$, and $\nu = 0,1$ for the Brownian ensembles of Gaussian and Wishart type, respectively.

The above equation clearly indicates the dependence of $\overline{\langle I_q(\Lambda_I)\rangle}$ on the spectral scale e and system size N. For finite but large Λ_I, it can further be approximated as $\overline{\langle I_q(\Lambda_I)\rangle} \approx \prod_{k=2}^{q}\frac{t_1(k)}{t_2(k)} + O(e^{-t_2\,\Lambda_I})$. With $\mathcal{K}_2 > \mathcal{K}_1 \gg 1$ (for large N), implying $t_2 \to 1$, the above gives $\overline{\langle I_2\rangle} \approx \frac{\beta+2}{\beta\,\xi}$, where ξ is the average localization length in case of the localized eigenfunctions: $\xi \approx \frac{1}{\langle|\Psi(r)|^2\rangle_e}$; this is in agreement with other studies [31]. Further note, for $\Lambda_I \to \infty$, $\overline{\langle I_q\rangle}$ approaches a correct steady-state limit, namely, XOE or XUE with X $\equiv$ L or G: $\overline{\langle I_q\rangle} = \frac{(2q)!}{2^q q!}N^{1-q}$ for $\beta = 1$ and $\overline{\langle I_q\rangle} = q!N^{1-q}$ for $\beta = 2$ [30].

As discussed in Ref. [14], the local intensity $\langle|\Psi(r)|^2\rangle_e$ (given by $N^{-1}\;\langle u(r)\rangle$ in Ref. [14]) depends on the perturbation strength $Y - Y_0$ of a BE and is different for Gaussian and Wishart ensembles. For later reference, here we mention the result for a Gaussian BE: $\langle|\Psi(r)|^2\rangle_e \propto \frac{1}{N\sqrt{Y-Y_0}}$. For a BE appearing during Poisson to GOE or GUE, and, with $Y - Y_0 \sim N^{-\gamma}$, this gives $\Lambda_I \sim \frac{N^{1-\gamma}}{E_c^2}$ and $\overline{\langle I_q\rangle} \sim N^{(\gamma-2)(q-1)/2}$ for $q > 0$. A comparison of the above result with $\overline{\langle I_q(\Lambda_I)\rangle} \sim N^{-\tau_q}$ then gives, for $q > 0$,

$$\tau_q \approx \tfrac{1}{2}(q-1)(2-\gamma). \tag{13}$$

This in turn implies all the fractal dimensions for large but finite Λ_I of the BE are same: $D_q \approx \frac{(2-\gamma)}{2}$.

B. Diffusion of multifractality spectrum

A well-known criteria for the multifractality is the singularity spectrum $f(\alpha)$: it is defined as the fractal dimension of set of those points r at which $|\psi(r)|^2 \sim N^{-\alpha/d}$ (with d as system dimension) and is related to τ_q by a Legendre transformation $f(\alpha) = q\alpha - \tau_q$. The number of such points in a lattice scales as $N^{f(\alpha)/d}$. Following from the definition, $f(\alpha)$ is a convex function and satisfies a symmetry $f(d-2\alpha) = f(\alpha) + d - \alpha$ [30]. This in turn implies a symmetry in anomalous dimension too: $\Delta_q = \Delta_{1-q}$.

For the delocalized wave functions $f(\alpha)$ is fixed: $f(\alpha) = d$ but its spread increases in crossover from the delocalized wave limit to the localized one. In case of an ensemble, $f(\alpha,e) = \lim_{N\to\infty} f(\alpha,e,N)$ can be expressed in terms of the distribution $P_u(u,e)$ of the local intensity $u = N\;|\psi|^2$ of a typical eigenfunction ψ [1],

$$f(\alpha,e,N) = \frac{d\;\ln(N\;u\;P_u(u,e))}{\ln N}, \tag{14}$$

where $\alpha = d(1 - \frac{\ln u}{\ln N})$ with d as the system-dimension and $P_u(u,e) = \frac{1}{N}\langle\sum_{k=1}^{N}\delta(u - N|z_{nk}|^2)\delta(e - e_k)\rangle$. For systems with weak multifractality, $f(\alpha)$ is believed to be approximately parabolic [30]: $f(\alpha) = d - \frac{1}{4\epsilon}(d + \epsilon - \alpha)^2 + o(\epsilon^4)$ with $\epsilon \ll 1$. This in turn implies $D_q \approx d - \epsilon\;q$. Note, $d = 1$ for a classical ensemble as well as BE.

For a classical ensemble, the eigenfunction are delocalized in the basis-space and $P_u(u) = \int P_u(u,e)\;de$ with $P_u(u)$ as a chi-square distribution [7]: $P_u(u) = \frac{e^{-u/2}}{\sqrt{2\pi u}}$ for XOE and $P_u(u) = e^{-u}$ for XUE (with X = G, L). The corresponding $f(\alpha)$ is then

$$f(\alpha,N) \approx 1 + \frac{\beta}{2}\left(1 - \alpha - \frac{N^{1-\alpha}}{\ln N}\right) + \frac{(\beta-2)}{2}\frac{\ln 2\pi}{\ln N}. \tag{15}$$

To derive Y-dependence of $f(\alpha,e,N)$ for a BE, we first invert the relation Eq. (14), which gives $P_u(u,e) = N^{\alpha-2+f} = e^{(\alpha-2+f)\ln N}$. As discussed in Ref. [14], a variation of the parameter Y gives rise to the diffusion of $P_u(u,e)$ (using the notation $\langle u\rangle_e = \frac{N}{\xi}$):

$$\frac{\partial P_u}{\partial Y} = 2\;\mathcal{K}_2\left[\frac{N}{\xi}\;\frac{\partial^2(u\;P_u)}{\partial u^2} + \frac{\beta}{2}\;\frac{\partial}{\partial u}\left(u - \frac{N}{\xi}\right)P_u\right] + L_e P_u, \tag{16}$$

where

$$L_e \equiv \frac{\partial}{\partial e}\left[\beta a(e) + \frac{2\beta\;N}{E_c}\;e^\nu + \frac{\partial}{\partial e}\;e^\nu\right], \tag{17}$$

with $a(e) = (\frac{2}{\beta})^\nu\;e + \frac{\nu}{2}(N - N_a - 1)$, E_c as the Thouless energy, and $\nu = 0,1$ for Gaussian and Wishart type Brownian ensembles, respectively.

A substitution of $P_u(u,e)$ as a function of $f(\alpha)$ in Eq. (16) leads to the diffusion equation for $f(\alpha)$:

$$\frac{\partial f_\alpha}{\partial\Lambda_f} \approx \frac{N^\alpha}{\xi}\left[\frac{1}{\ln N}\;\frac{\partial^2 f_\alpha}{\partial\alpha^2} + \left(\frac{\partial f_\alpha}{\partial\alpha}\right)^2 + \frac{\partial f_\alpha}{\partial\alpha}\left(1 + \frac{\beta}{2} - \frac{\beta}{2}\frac{\xi}{N^\alpha}\right)\right] + \frac{\beta}{2}\frac{N^\alpha}{\xi} + T_e f_\alpha, \tag{18}$$

with

$$\Lambda_f = \frac{2\;\mathcal{K}_2\;(Y - Y_0)}{\ln N}, \tag{19}$$

where T_e is the differential operator

$$T_e f_\alpha \equiv \frac{\ln N}{2\;\mathcal{K}_2}\left\{\frac{\beta\;\phi_\nu}{\ln N} + [\beta\;(\phi_\nu\;e + \theta_\nu) + 2\;\nu]\;\frac{\partial f_\alpha}{\partial e} + e^\nu\;\frac{\partial^2 f_\alpha}{\partial e^2} + \ln N\;e^\nu\left(\frac{\partial f_\alpha}{\partial e}\right)^2\right\}, \tag{20}$$

where θ_ν,ϕ_ν depend on the nature of BE: $\theta_0 = \frac{2N}{E_c}, \phi_0 = 1$ for Gaussian BEs, $\theta_1 = \frac{N-N_a-1}{2}, \phi_1 = \frac{2}{\beta} + \frac{2N}{E_c}$ for Wishart BEs. The appearance of $T_e f$ in Eq. (18) clearly indicates an energy-sensitivity of the multifractality spectrum: it is nonstationary along the energy axis.

A desirable next step would be to solve the above equation but it is technically complicated. To gain further insight, we first simplify Eq. (18) by a local spectral averaging, which gets rid of the $T_e f$: integrating Eq. (18) over the energy range $e - \Delta e \to e + \Delta e$, while assuming f to be locally stationary over the region, leads to

$$\frac{\partial \overline{f}_\alpha}{\partial \Lambda_f} \approx \frac{N^\alpha}{\xi}\left[\frac{1}{\ln N}\frac{\partial^2 \overline{f}_\alpha}{\partial \alpha^2} + \overline{\left(\frac{\partial f_\alpha}{\partial \alpha}\right)^2} + \frac{\partial \overline{f}_\alpha}{\partial \alpha}\left(1+\frac{\beta}{2}\right) + \frac{\beta}{2}\right] - \frac{\beta}{2}\left(\frac{\partial \overline{f}_\alpha}{\partial \alpha} - \frac{\phi_\nu}{\mathcal{K}_2}\right), \tag{21}$$

where $\overline{f}_\alpha = \frac{1}{2\Delta e}\int_{e-\Delta e}^{e+\Delta e} f_\alpha \, de$. Based on size-dependence of ξ, the above equation can further be reduced to a simple form. Noting that $\xi \propto (\langle I_2 \rangle)^{-1} \propto N^{D_2}$ in the spectrum-bulk, with $0 \leqslant D_2 \leqslant 1$, we can approximate, for $N^\alpha \ll \xi$, or equivalently for $\alpha < D_2 \leqslant 1$,

$$\frac{\partial \overline{f}_\alpha}{\partial \Lambda_f} \approx -\frac{\beta}{2}\left(\frac{\partial \overline{f}_\alpha}{\partial \alpha} - \frac{\phi_\nu}{\mathcal{K}_2}\right). \tag{22}$$

This indicates a linear α dependence of $f(\alpha)$ for regions $\alpha < D_2$: $\overline{f}_\alpha = l_0 + l_1\,\alpha$, where $l_0(\Lambda_f)$ and $l_1(\Lambda_f)$ depend on the initial conditions: $l_0(\Lambda_f) = \frac{\beta}{2}\,(\frac{\phi_\nu}{\mathcal{K}_2} - l_1)\Lambda_f + l_0(0)$ and $l_1 =$ constant.

For regions where $\alpha \gg D_2$, the first term with square bracket of Eq. (21) dominates the second term. This in turn leads to the following condition on the possible solution:

$$\frac{1}{\ln N}\frac{\partial^2 \overline{f}_\alpha}{\partial \alpha^2} + \overline{\left(\frac{\partial f_\alpha}{\partial \alpha}\right)^2} + \frac{\partial \overline{f}_\alpha}{\partial \alpha}\left(1+\frac{\beta}{2}\right) + \frac{\beta}{2} = 0. \tag{23}$$

Thus, $\overline{f}_\alpha$ now must satisfy both Eq. (22) as well as Eq. (23) simultaneously; one possible solution in this case seems to be $\overline{f}_\alpha = h_0 + h_1\alpha$ with $h_0 = -\frac{\beta}{2}(h_1 - \frac{\phi_\nu}{\mathcal{K}_2})\Lambda_f + h_0(0), h_1 = -\frac{\beta}{2}, -1$. A linear α-dependence of $\overline{f}_\alpha$ was indicated also by a previous study [1] in context of BEs appearing between Poisson to GOE.

As mentioned above, previous studies of multifractal states have suggested a parabolic solution for f_α in weak multifractality regime (with $D_2 \approx 1 - 2\epsilon$). Following from Eq. (18), such a solution can exist in a small neighborhood of $\alpha \sim 1 - 2\epsilon + s$ with s given by the size dependence of Λ_f: $\Lambda_f = \Lambda_0\, N^{-s}$. This can be seen by a substitution of $f_\alpha = v_0 + v_1\,\alpha + v_2\,\alpha^2$ in Eq. (18) directly (assuming local stationarity), which gives $v_0(\Lambda_f) = \frac{2c}{ln N}\, ln(\frac{1}{v_2(0)} - \lambda_f) + \frac{cx(v_1(0)^2)}{1-x\Lambda_f} + (\frac{\beta c}{2} + \frac{\beta\,\phi_\nu}{2\mathcal{K}_2} - c{d_0}^2)\lambda_f, v_1(\Lambda_f) = \frac{(v_1(0)\,+\,d_0)x}{1-x\lambda_f} + d_0, v_2(\Lambda_f) = \frac{v_2(0)}{1-x\lambda_f}$, where $c = N^{\alpha-D_2} = N^s$, $x = 4cv_2(0)$, $d_0 = \frac{\beta+2}{4} - \frac{\beta}{4c}$, and $v_k(0)$ with $k = 0,1,2$ corresponding to initial conditions.

C. Diffusion of wave-function correlations

As intuitively expected, the anomalous scaling behavior of the multifractal states is also reflected by the overlap of their intensities. For example, during metal-insulator transition, two wave functions, say $\Psi(r)$ and $\Psi'(r')$, are known to display the following correlation: $N^2\langle|\Psi^2(r)\Psi'^2(r')|\rangle \sim \frac{(|r-r'|}{L_\omega)}^{\Delta_q}$ for $|r-r'| < L_\omega$ with Δ_q as the anomalous dimension, $L_\omega \sim (\rho\omega)^{-1/d}$, $\omega = |e_i - e_j|$, ρ as the average level density, and d as the system dimension [30]. It is therefore natural to seek the role of the correlations in context of criticality in BEs [30].

The two-point intensity correlation $C(e',e'')$ between two eigenstates, say Ψ_a and Ψ_b, with eigenvalues e_a, e_b, respectively, for a $N \times N$ matrix H, can be defined as

$$C(e',e'') = \sum_{a,b}\sum_{m=1}^{N} |\Psi_{ma}|^2\,|\Psi_{mb}|^2\,\delta(e'-e_a)\delta(e''-e_b) \tag{24}$$

(with Ψ_{ma} implying mth component of the eigenfunction Ψ_a). As intuitively expected, its ensemble average is related to the two-point spectral correlation $R_2(e',e'')$. This in turn connects the eigenfunction statistics in the critical regime to that of eigenvalues. As discussed in Ref. [14] for BEs, the perturbation by a stationary ensemble leads to an evolution of $\langle C(e,\omega)\rangle$ from an arbitrary initial condition, which depends on both e,ω (with $e' = e + \omega, e'' = e - \omega$) and is nonstationary. But for the local correlations, i.e., those for which a variation with respect to e can be ignored, the Y-governed evolution can be approximated as

$$2\,\frac{\partial\langle C\rangle}{\partial \Lambda_e} \approx \left[\frac{\partial^2}{\partial r^2} + \beta\frac{\partial}{\partial r}\left(2\eta\, r + \frac{1}{r}\right) - \frac{(\beta+2)}{2\,r^2} + 2\beta\eta\right]\langle C\rangle + \frac{\beta}{4\,r^2}\,\langle I_{2(r_0+r)} + I_{2(r_0-r)}\rangle\; R_2(r_0,r), \tag{25}$$

where $\eta = \mathrm{e}^{-\nu}\,\Delta_\mathrm{e}^2\,\beta_2$ with $\beta_2 = [(\frac{2}{\beta})^\nu + \frac{\nu N}{E_c}]$, $\nu = 0,1$ for Gaussian BE and Wishart BE, respectively, r_0, r are the rescaled energy $e = r_0\,\Delta_e, \omega = r\,\Delta_e$, with Λ_e defined in Eq. (1) and $I_{2,r}$ is the second inverse participation ratio at energy r.

In the stationary limit $\Lambda_e \to \infty$, it is easy to check that $\langle C\rangle = R_2(r_0,r)$ (using the relation $\langle I_{2,r_0}\rangle = \frac{(2+\beta)}{\beta N}$ for the stationary ensembles with ergodic eigenfunctions). An exact solution of the above equation for finite, nonzero Λ_e is complicated, but, for small-r, it can be obtained by expanding $\langle C\rangle$ in Taylor's series around $r = 0$. As discussed in Ref. [14], the small-r behavior of $\langle C\rangle$ depends on the small-r behavior of $R_2(r)$. For bulk regions where $\langle I_2(r)\rangle$ is almost constant and $R_2(r) \propto r^\beta$, one has $\langle C\rangle \propto r^\beta$.

For criticality considerations, an asymptotic behavior of $\langle C\rangle$ is relevant, which can be given as $\langle C\rangle = r^{-t}\,\sum_{n=0}^{\infty} c_n(\Lambda_e)\,r^{-n}$, with coefficients c_n dependent on initial conditions and energy-range r_0. For r_0 in the bulk of spectrum, $I_{2,r_0+r} = I_{2,r_0-r} \approx I_{2,r_0}$ is almost constant. Neglecting the terms containing η, due to being $o(1/N)$ smaller as compared to other terms (note $\eta \propto \Delta_e^2$), this leads to three possible solutions corresponding to $t = 0,1,2$:

$$\langle C\rangle = \frac{1}{r^t}\left[c_0(\Lambda_e) + \frac{c_1(\Lambda_e)}{r} + O\left(\frac{1}{r^2}\right)\right], \tag{26}$$

where (i) $c_0(\Lambda_e) = c_0(0), c_1(\Lambda_e) = c_1(0)$ for $t = 0$, (ii) $c_0(\Lambda_e) = c_0(0), c_1(\Lambda_e) = (c_1(0) + \frac{\beta}{4}\int_0^{\Lambda_e} I_2\, d\Lambda_e)$ for $t = 1$,

(iii) $c_0(\Lambda_e) = (c_0(0) + \frac{\beta}{4}\int_0^{\Lambda_e} I_2\, d\Lambda_e)$, $c_1(\Lambda_e) = c_1(0)$ for $t = 2$. Higher c_n are given by the recursion relation

$$c_{n+2}(\Lambda_e) = e^{\beta\eta\Lambda_e/2}\left[c_{n+2}(0) + \frac{\beta}{4}\int_0^{\Lambda_e} g(\Lambda_e)\, d\Lambda_e\right], \quad (27)$$

where $g(\Lambda_e) = [2(n+t+\beta+1)(n+t) + (\beta-2)]\, c_n(\Lambda_e) + \beta\, I_{2,r_0}\, \delta_{n0}\, \delta_{t0}$, where δ_{uv} is the Kronecker δ function: $\delta_{uv} = 1$ or 0 for $u = v$ and $u \neq v$, respectively.

As discussed above, $\langle C(r_0,r)\rangle \to R_2(r_0,r)$ for small r. It is therefore appropriate to consider the measure $K(r) = \frac{\langle C(r)\rangle}{R_2(r)}$ as the criteria for criticality: $K(r) \to 1$ for $r < 1$ and is universal but is system-dependent for $r > 1$ (as in this case $R_2 \to 1$ leading to $K(r) \to \langle C(r)\rangle$). For criticality considerations, therefore, the large-r behavior is relevant. For many systems undergoing the localization-to-delocalization transition of eigenstates, the behavior of $K(r)$ for $r > 1$ is described by the Chalker's scaling [32]: $K(r) \sim r^{D_2-1}$ but $K(r) \sim r^{-2}$ for r of the order of spectral band width [33]. But, as clear from the above, the large r behavior of $K(r)$ for a BE depends on the initial conditions as well as location of the spectral scale e; here, $K \sim \frac{1}{r^2}$ behavior can occur for $r > 1$ in the bulk spectral regimes (as here the ensemble averaged inverse participation ratio is almost energy-independent). For BE cases near the edge or intermediate spectral region, $K \sim \frac{c_0}{r^t} + O(r^{t+1})$ with t determined by the energy-dependence of the inverse participation ratio I_2.

For critical BE cases, Λ_e is N-independent and some of the higher c_n may become larger than c_0. The $K(r)$ behavior in the range $r \sim o(1)$ around r_0 is then dominated by $\frac{1}{r^n}$ term. As an example, we consider the BE case with Poisson initial condition and in the bulk of spectrum for cases with $I_2 = N^{-D_2}$ with $D_2 < 1$ and $E_c \sim 1$. As for Poisson limit $\langle C\rangle = \frac{1}{N}$ [33], this implies $t = 0$, $c_0(0) = \frac{1}{N}$, $c_n(0) = 0$ for $n > 0$. From the above, we then have $c_0(\Lambda_e) = \frac{1}{N}$, $c_2(\Lambda_e) = \frac{\beta\Lambda_e}{4}N^{-D_2}$, $c_{2n}(\Lambda_e) \sim (\Lambda_e)^n\, N^{-D_2}$ for $n > 1$ and $c_{2n+1}(\Lambda_e) = 0$ for $n \geqslant 0$. For a size-dependent Λ_e, say $\Lambda_e \sim N^{-a}$, such that $D_2 + a < 1$, therefore, the dominant contribution comes from the terms r^{-2}, which leads to $K(r,\Lambda_e) \sim \frac{1}{r^2}$ for $r \sim o(1)$. But for a size-independent Λ_e, c_n rapidly increase with n for $n > 2$; this in turn leads to $K(r,\Lambda_e) \sim \frac{1}{r^t}$ with t subjected to the condition $c_{t+1} < r\, c_t$ and c_t given by Eq. (27).

V. CRITICAL BE DURING POISSON → GOE TRANSITION: NUMERICAL ANALYSIS

The theoretical results in Secs. II–IV are applicable to the critical Brownian ensembles of both Gaussian and Wishart type. For the numerical analysis, however, we focus on a specific Gaussian BE, namely, the one that appears during Poisson to GOE crossover (due to its relevance in context of localization to delocalization transition of the eigenfunctions).

Consider the transition in Gaussian ensembles with an initial state $H = H_0$ described by the ensemble density $\rho_0(H_0) \propto e^{-\sum_i H_{0;ii}^2}$. For a complete localization of its eigenfunctions in the basis in which H_0 is represented, the initial spectral statistics belongs to the Poisson universality class. The perturbation, of strength λ, by a matrix V taken from a GOE (when represented in the unperturbed basis and of variance $v^2 = 1$), subjects eigenfunctions to increasingly

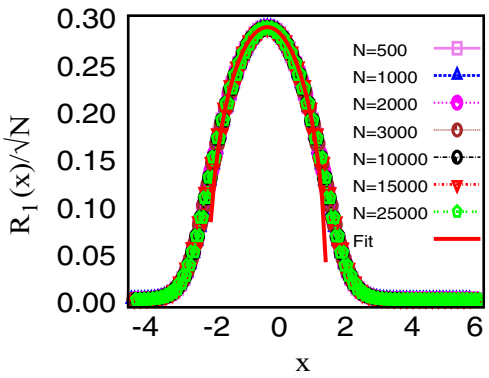

FIG. 1. Ensemble-averaged level density $R_1(x)$: Behavior of the Brownian ensemble (BE) Eq. (28), with $\mu = N$ for many system sizes N, where $x = e/\sqrt{N}$; here, $R_1(x)$ for different N is scaled by $\sqrt{N}$. The solid line corresponds to the fit—$R_1(e) = \frac{1}{b\pi}\sqrt{2bN - e^2}$ with $b \approx 2$, confirming the semicircle behavior at bulk. The behavior near the edge is deviating from semicircle fit but collapse of $R_1(x)$ for different N on the same curve indicates same N-dependence for all energy ranges: $R_1(e) = \sqrt{N} f(e/\sqrt{N})$. A comparison of $R_1(e)$ with spectral level density $\rho_{\rm sm}(e)$ is given in Ref. [18].

delocalize as a function of λ. The ensemble of matrices $H = \sqrt{f}(H_0 + \lambda V)$, with $f = (1+\lambda^2)^{-1}$ then corresponds to the Brownian ensemble during Poisson → GOE transition; it is described by the probability density [15,25,26,34–36],

$$\rho(H) \propto \exp\left[-\frac{\gamma_b}{2}\sum_{i=1}^{N} H_{ii}^2 - 2\gamma_b(1+\mu)\sum_{i,j=1;i<j}^{N}|H_{ij}|^2\right], \quad (28)$$

with $2(1+\mu) = (\lambda^2 f)^{-1}$ and arbitrary γ_b; here, $H = H_0$ for $\lambda \to 0$ or $\mu \to \infty$ and $H = V$ for $\lambda \to \infty$ or $\mu \to 0$. As mentioned in Sec. II, the evolution of matrix elements is described in terms of the parameter $Y = -\frac{1}{2}\log f$, which in this case becomes $Y \approx \frac{1}{2\mu}$.

The standard route for the spectral statistical analysis is based on the fluctuations around the average level density. In the present case, the ensemble averaged level density $R_1(e)$, also known as first-order spectral correlation, changes from a Gaussian to a semicircular form at the scale of $N\mu \sim R_1^2$: $R_1(e) = \frac{N}{\sqrt{\pi}}e^{-e^2}$, $\frac{1+\mu}{\pi}\sqrt{\frac{2N}{1+\mu} - e^2}$, $NF(e,a)$ for $(\mu/N) \to \infty, 0, a$, respectively [34], with a as an N-independent constant. Although the exact form of the function $F(e,a)$ is not known, our numerical analysis, displayed in Fig. 1, suggests a semicircle behavior in the spectral bulk, i.e., $F(e) \approx (Nb\pi)^{-1}\sqrt{2bN - e^2}$ with Gaussian tails and b as a constant independent of N. (Note the study in Ref. [34] gives $R_1(e)$ for H as a complex Hermitian matrix but the numerical evidence given in Ref. [5] and in the present study confirms its validity also for the real-symmetric H.) Clearly, $R_1(e)$ is nonstationary as well as nonergodic [37]; as discussed below, this plays a crucial role in compressibility calculation.

As mentioned in Sec. II, the spectral fluctuations around $R_1(e)$ are governed by the parameter Λ_e [5], given by Eq. (1), which in this case becomes, with $Y - Y_0 = \frac{1}{2\mu}$ and mean level

spacing $\Delta_e(e) = R_1(e)^{-1}$,

$$\Lambda_e(e) = \frac{R_1^2(e)}{2\mu}. \tag{29}$$

For finite N, the Λ_e-variation due to changing μ at a fixed energy e results in a crossover of the spectral statistics from Poisson ($\Lambda_e \to 0$) to GOE ($\Lambda_e \to \infty$) universality class. In limit $N \to \infty$ and for arbitrary μ, $\Lambda_e(e)$ varies abruptly, approaching either 0 or ∞, ruling out the possibility of any intermediate statistics. But if μ takes a value such that the limit $\Lambda^*(e) \equiv \lim_{N\to\infty} \Lambda_e(e)$ exists, the statistics is then size-independent and belongs to a new universality class, different from the two end-points, and is referred to as the critical Brownian ensemble. As N-dependence of R_1 also varies with μ, this implies the existence of two critical points (instead of one as previously discussed in [15,34]):

$\mu = c_2 N$: as mentioned above, $R_1(e)$ for this case behaves as a semicircle in the bulk: $R_1(e) = (b\pi)^{-1}\sqrt{2bN - e^2}$. Although the behavior near the edge is not known, the numerical analysis, displayed in Fig. 1 for $c_2 = 1$, indicates a $\sqrt{N}$-scaling behavior in all regions: $\frac{1}{\sqrt{N}} R_1(\frac{e}{\sqrt{N}})$ is N-independent. Equation (29) then gives

$$\Lambda_e(e) = \frac{2bN - e^2}{2\pi^2 b^2 N c_2}, \tag{30}$$

with $b \sim 2$. Note, for $c_2 = 1$, although $\Lambda_e(e)$ is size-independent near the band-center $e \sim 0$, it is still quite large ($\Lambda_e \approx \frac{1}{2\pi^2}$), indicating the level-statistics to be close to the GOE. An intermediate statistics between Poisson and GOE can, however, be seen near $e \sim e_0\sqrt{N}$ for $e_0 \approx 1.7 < b$.

As mentioned in Sec. IV A, $\xi \sim N\sqrt{Y - Y_0}$ for Gaussian-type BEs, which gives, for this case, $\xi \approx \frac{N}{\sqrt{2\mu}} \sim N^{1/2}$ and $\langle I_2\rangle \sim \xi^{-1} \sim N^{-1/2}$ in the bulk. This further implies $\tau_2 = D_2 = 0.5$ and $\chi = (1 - D_2)/2 = 0.25$ for the spectrum bulk, which is in near agreement with our numerical result [which gives $\tau_2 \approx 0.6$ and $\chi \approx 0.2$, see Fig. 6(b)].

$\mu = c_1 N^2$: as here $\lim_{N\to\infty} \frac{\mu}{N} \to \infty$, R_1 now becomes $\frac{N}{\sqrt{\pi}}\, e^{-e^2}$. From Eq. (29), Λ_e is again size-independent:

$$\Lambda_e(e) = \frac{1}{2\pi c_1} e^{-2e^2}. \tag{31}$$

For $c_1 \sim 1$, $e \sim 0$, $\Lambda_e \sim \frac{1}{2\pi}$, and the statistics lies between Poisson and GOE even for energy ranges near $e \approx 0$. As here $Y - Y_0 \propto N^{-2}$, this gives $\xi \sim N^0 = O(1)$, $\langle I_2\rangle \sim N^0$, $D_2 \sim 0$, which suggest a strong multifractal behavior (approaching localization) of the eigenfunctions (note the latter rules out the validity of the relation $D_2 = 1 - 2\chi$ in this case).

The theoretical formulations of the spectral compressibility and multifractal spectrum discussed in previous sections are based on a few approximations at various stages of the derivation. It is therefore desirable to verify the results by numerical route. The latter can also give an insight in critical point behavior of some other measures e.g nearest neighbor spacing distribution. The numerical evidence for the criticality for the case $\mu \propto N^2$, with H taken from a real-symmetric ensemble or complex-Hermitian ensemble, is discussed and verified in Ref. [5]. The criticality of BE for this case but H taken from a real-quaternion ensemble was numerically verified in Ref. [23] (see Fig. 3 of Ref. [23]). In the present work, we pursue a numerical analysis of the case $\mu \propto N$ only. To understand the non-stationary aspects of critical statistics, we analyze three energy regime, i.e., edge, bulk ($e \sim 0$), or at intermediate energies (the region where $R_1(e)$ is half of its maximum value). Although, due to rapid change in $R_1(e)$, the edge results are believed to be error-prone and thus a bit unreliable, but our results show a systematic trend which encourages us to include them in the figures here.

A. Critical spectral statistics

Our theoretical claim about criticality of BE at $\mu = c_2 N$ is based on a $\sqrt{N}$-dependence of the average level density R_1. Our first step is therefore to numerically confirm its size-dependence. At this stage, an important question is regarding the ergodicity of the level density for the BE which implies $\rho_{\rm sm}(e) = R_1(e)$, with $\rho_{\rm sm}$ as the spectral averaged level density; $R_1(e)$ can then be used as a substitute for $\rho_{\rm sm}(e)$ for various analytical purposes [37]. The ergodicity is confirmed in a previous study [18] (by a numerical comparison of the ensemble and the spectral averaging of the level density). It is therefore sufficient to analyze the size-dependence of $R_1(e)$. For this purpose, we consider the ensembles consisting of a large number of real-symmetric matrices, for many matrix sizes with $c_2 = 1$; the spectrum for each such ensemble is numerically generated using LAPACK subroutine based on an exact diagonalization approach. As shown in Fig. 1, $R_1(e)$ is indeed semicircle in the bulk but deviating from it near the edge. Further, the N-dependence is the same for all energy ranges, including edge as well as bulk.

As a next step, we analyze the spectral statistics, which requires a careful unfolding of the spectrum. Due to unavailability of the analytical form of $R_1(e)$ for all energy ranges, we apply the local unfolding procedure [29] based on following steps: the smoothed level density $\rho_{\rm sm}$ for each spectrum is first determined by a histogram technique and then integrated numerically to obtain the unfolded eigenvalues $r_n = \int_{-\infty}^{e_N} \rho_{\rm sm}\, de$. The spectrum being nonstationary with energy-sensitive fluctuations (see Figs. 2 and 3 of Ref. [18]), it is necessary to analyze the statistics at different energy-ranges. For Λ_e-based comparisons, ideally one should consider an ensemble averaged fluctuation measure at a given energy-point e without any spectral averaging. But in the regions where Λ_e varies very slowly, it is possible to choose an optimized range Δe, sufficiently large for good statistics but keeps mixing of different statistics at minimum. We analyze 5% of the total eigenvalues taken from a range Δe, centered at the energy-scale of interest, i.e., edge, bulk, and intermediate energies. (As for $\mu = c_2 N$ ($c_2 = 1$), $\rho_{\rm sm}$ in the bulk is almost constant, the statistics is locally stationary, and one can take levels within larger energy ranges without mixing the statistics. A rapid variation of $\rho_{\rm sm}$ in the edge, however, permits one to consider the levels within very small spectral ranges only. For edge-bulk comparisons, it is preferable to choose the same number of levels for both spectral regimes.) The number of matrices M in the ensemble for each matrix size N is chosen so as to give approximately 10^5 eigenvalues and their eigenfunctions for the analysis.

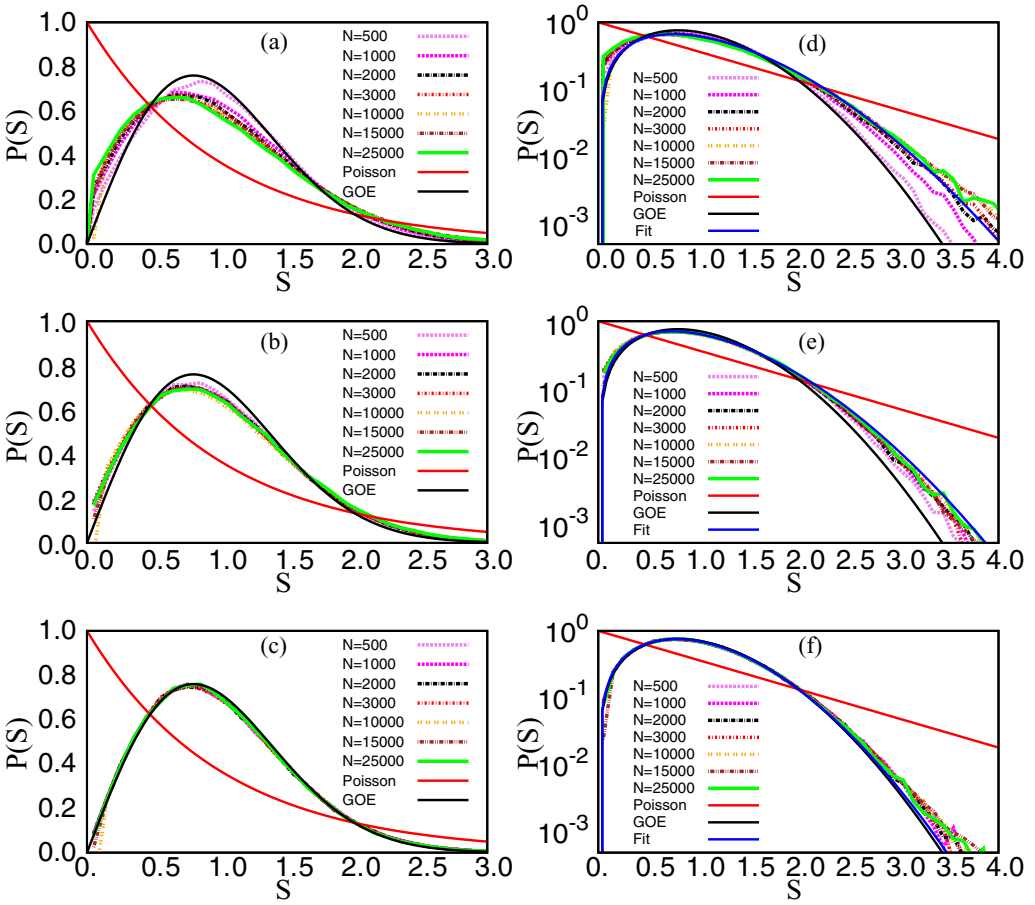

FIG. 2. Nonstationarity of $P(s)$: Nearest-neighbor spacing distribution for the ensemble density Eq. (28), with $\mu = N$ for many system sizes N in three energy ranges: (a, d) edge [neighbourhood of minimum $R_1(e)$], (b, e) intermediate [the neighborhood where $R_1(e)$ is half of its maximum value], (c, f) bulk [neighborhood of maximum $R_1(e)$]. Sensitivity of $P(S)$ to the energy can be seen from the small "s" behavior (a–c) and large "s" behavior (d–f). As clear from panels (a) and (d), deviation of $P(s)$ from GOE increases as N increases. The behavior in the bulk is close to GOE limit, but the one in the intermediate regime is different from both Poisson and GOE limit [the difference is more clear in panel (e), although it can also be seen in panel (b) near $S \sim 1$]; as $\Lambda_{\rm bulk} > \Lambda_{\rm intermediate} > \Lambda_{\rm edge}$, the above shift of statistics from GOE is in agreement with theoretical prediction. As expected for the critical statistics, $P(s)$ in (b) approaches an invariant form with increasing system size N. Panels (d), (e), and (f) also compare the tail behavior with the fit $[a\ s\ \exp(-bs^2 - \kappa s)]$, with $a = 1.9$, $b = 0.42$, $\kappa = 0.70$ for edge, $a = 2.01$, $b = 0.47$, $\kappa = 0.66$ for intermediate regime, $a = 1.7$, $b = 0.73$, $\kappa = 0.154$ for bulk.

To verify size-independence of the spectral statistics for $\mu \propto N$, we consider $P(s)$ and $\Sigma_2(r)$ for the BE with $\mu \propto N$ for many system sizes. For comparison, it is useful to give their behavior in the two stationary limits:

(i) *GOE:* $P(s) = \frac{\pi}{2}\ s\ \exp(-\pi s^2/4), \Sigma_2(r) = \frac{2}{\pi^2}\ (\ln r + C)$, with $C \approx 2.18$,

(ii) Poisson: $P(s) = \exp(-s), \qquad \Sigma_2(r) = r.$

It is desirable to compare the BE-numerics with theoretical BE results too but the exact $P(s)$ behavior for the BE with matrices of arbitrary size N is not known. It is, however, easy to derive the $P(s)$ for $N = 2$ case [36,38]: $P(s,\Lambda) \approx (\frac{\pi}{8\Lambda})^{1/2}\ s\ e^{-s^2/16\Lambda}\ I_0(\frac{s^2}{16\Lambda})$, with I_0 as the modified Bessel function. As $P(s)$ is dominated by the nearest neighbor pairs of eigenvalues, this result is a good approximation also for $N \times N$ case, especially in the small-s and small-Λ result [36].

Figures 2, 3, and 4 display the behavior of $P(s)$ and $\Sigma_2(r)/r$ for the BE case $\mu = N$ for many system sizes ranging from $N = 500$ to $N = 25\,000$, in three energy regions. With $R_1(e) \propto \sqrt{N}$ for arbitrary e (see Fig. 1), Λ_e [given by Eq. (30)] in this case is N-independent but its value varies from edge to bulk: $\Lambda_e(e \sim 2.5\sqrt{N}) < \Lambda_e(e \sim 1.7\sqrt{N}) < \Lambda_e(e \sim 0)$. As a consequence, the statistics is expected to be critical (i.e., intermediate between Poisson and GOE) but different in the three spectral regimes. This is indeed in agreement with the behavior of the measures shown in Figs. 2, 3, and 4. For $e \sim 0$, the statistics is nearer to GOE regime [Figs. 2(c), 2(f) 3(c), 4(c), and 4(f)], but its deviation from GOE increases for $e \sim e_0\sqrt{N}$ case with $e_0 \sim 1.7$ [Figs. 2(b), 2(e) 3(b), 4(b), and 4(e)]. For e near the edge, the statistics is expected to be closer to Poisson limit. Although this is confirmed by the tail behavior of $P(s)$ shown in Fig. 2(d) and $\Sigma_2(r)/r$ in Figs. 3(a), 4(a) and 4(d), the small-s behavior of $P(s)$ is still far from Poisson limit [Fig. 2(a)]. This clearly indicates the dependence of the speed of transition on the spectral ranges: although Λ_e is small in this regime but for spectral ranges $\delta e < \Lambda_e$, the transition to GOE is almost complete.

The study in Ref. [19] suggests that an exponential decaying tail of the $P(s)$ is an indicator for the critical spectral

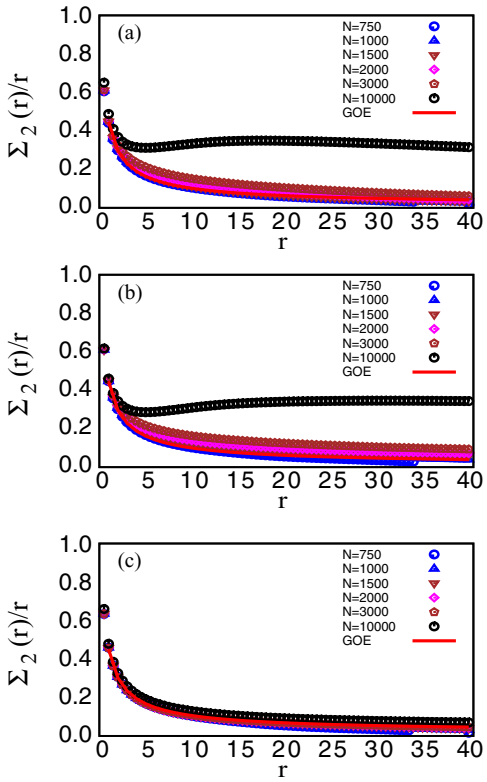

FIG. 3. Nonstationarity of compressibility $\Sigma_2(r)/r$: Variance of number of levels in a distance of r mean level spacings for the BE, Eq. (28), with $\mu = N$ for many system sizes in three energy ranges: (a) edge, (b) intermediate, and (c) bulk. The solid line in panels (a), (b), and (c) corresponds to the theoretical prediction for GOE mentioned in Sec. V A. As indicated by panels (a) and (b), the critical behavior of χ (i.e., $0 < \chi < 1$) is not evident for small N cases but appears only in large N limit (note, however, an upward shift of the curves, although very small, can be seen even for small N). This is caused by the spurious fluctuations due to finite-size effects, expected to be more pronounced in the large r limit. This is analyzed in more detail in Fig. 4.

statistics. Figures 2(d)–2(f) show a comparison of the tail behavior of $P(s)$ with the curve $P(s) = a\ s\ \exp(-bs^2 - \kappa s)$, where $\kappa \sim 0.70, 0.66,$ and 0.154 for levels taken from the edge, intermediate, and bulk, respectively. (Note, the fit is a close approximation of the theoretical formulation for $P(s)$ mentioned above for a 2×2 BE.)

The compressibility χ can be numerically obtained from the large-r limit of $\Sigma_2(r)/r$ curves in Figs. 3 and 4; the numerical result is closer to our theoretical prediction $\chi = 1 - 4\sqrt{2}\,\pi\,\Lambda^*(e)$ [from Eq. (9)]. Using $\Lambda^*(e) = \frac{(4-e_0^2)}{8\pi^2}$ [from Eq. (30)], we get $\chi = 0.11$ and 0.75 for the bulk ($e_0 = 0$) and intermediate regime ($e_0 \approx 1.7$), respectively. (The lack of information about exact R_1 in the edge handicaps us from a theoretical prediction for Λ_e and therefore χ.) The small deviations from theory for smaller N can be attributed to the spurious fluctuations due to finite-size effects, which affects the long-range statistics more severely. The true fluctuations are expected to be seen by going to $N \to \infty$ limit. As can be seen from Fig. 4, $\Sigma_2(r)/r$ for $N = 25\,000$ are closer to theory than $N = 10\,000$. Note the bulk-value of $\chi \approx 0.11$ is expected on the basis of relation $\chi = (1 - D_2)/2$ too (valid for weak multifractal states in the bulk) [32]; the latter gives $\chi \approx 0.2$ with our numerically obtained $D_2 \approx 0.6$. For partially localized states, χ has been suggested to be related to exponential decay of $P(s)$ too [19]: $\chi \approx \frac{1}{2\kappa}$; using $\kappa \approx 0.66$ for intermediate regime $e \sim 1.7\sqrt{N}$ [given by P(s) fitting mentioned above], this gives $\chi \approx 0.75$, which is again in agreement with our theory. (Note the range of validity of the relations $\chi \approx \frac{1}{2\kappa}$ and $\chi = (1 - D_2)/2$ is different; the former is not applicable in near GOE regime and the latter is not valid in strong multifractal regime.)

It must be emphasized that $\Sigma_2(r)$ results are sensitive to the number of levels used for the analysis and the ensemble size M even for $N \sim 2.5 \times 10^4$; Fig. 4 displays the change in behavior for different number of levels taken from a given regime for a given N. As the compressibility calculation is based on a large r limit of $\frac{\Sigma_2(r)}{r}$, its numerical evaluation for the ensembles of BE type (with rapidly changing level density) cannot be reliable.

B. Multifractality analysis of wave functions

Our next step is to investigate the wave-function statistics based on standard measures, i.e., inverse participation ratio (IPR), singularity spectrum, and wave-function correlations at two different energies.

In the past, it has been conjectured that the distribution of I_q normalized to its typical value $I_q^{\rm typ} = \exp\langle \ln I_q \rangle$ has a scale-invariance at the localization-delocalization transition. This corresponds to a shape-invariance of $P(\ln I_q)$ with increasing system size N, the latter causing only a shift of the distribution along I_q axis [30]. The above conjecture was questioned at first but confirmed later by numerical studies on Anderson transition for $d > 2$ case (with d as dimension) and critical PRBM. To check its validity in case of the critical BEs, we numerically analyze the eigenstates for the case $\mu = N$. To overcome finite-size effects, one has to consider averages over different realizations of disorder as well as a narrow energy range. As these fluctuations in bulk are analyzed in detail in Ref. [1], here we confine ourselves to intermediate regime only. For this purpose, we consider the eigenstates in a narrow energy range 5% around intermediate energy for each matrix of the ensemble with $\mu = N$, consisting of M matrices, with $M = 8000, 6000, 5000, 3000, 2500, 1500$ for $N = 500, 750, 1000, 1500, 2000, 3000,$ respectively. Figure 5(a) shows the distribution $P(\ln I_2)$ for the critical BE with $\mu = N$; the scale invariance of the distribution is clearly indicated from the figure. As indicated by previous studies [30], the I_q-distribution is expected to show a power-law tail at the transition: $P(I_q/I_q^{\rm typ}) \propto (I_q/I_q^{\rm typ})^{-1-x_q}$ for $I_q \gg I_q^{\rm typ}$; the behavior is confirmed in Fig. 5(d) for $q = 2$ with $x_{q=2} \gg 1$ (our numerics gives $x_2 \sim 100$; however, a more detailed analysis is needed due to huge errors possible in tail of the distribution). Furthermore the change in peak-position of $P(\ln I_2)$ with changing system size confirms a power-law dependence of $\langle I_2 \rangle$ on system size N, governed by a continuous set of exponents: $\langle I_2 \rangle \sim N^{-\tau_2^{\rm typ}}$, where $\tau_2^{\rm typ} = \tau_2$ for $x_2 > 1$.

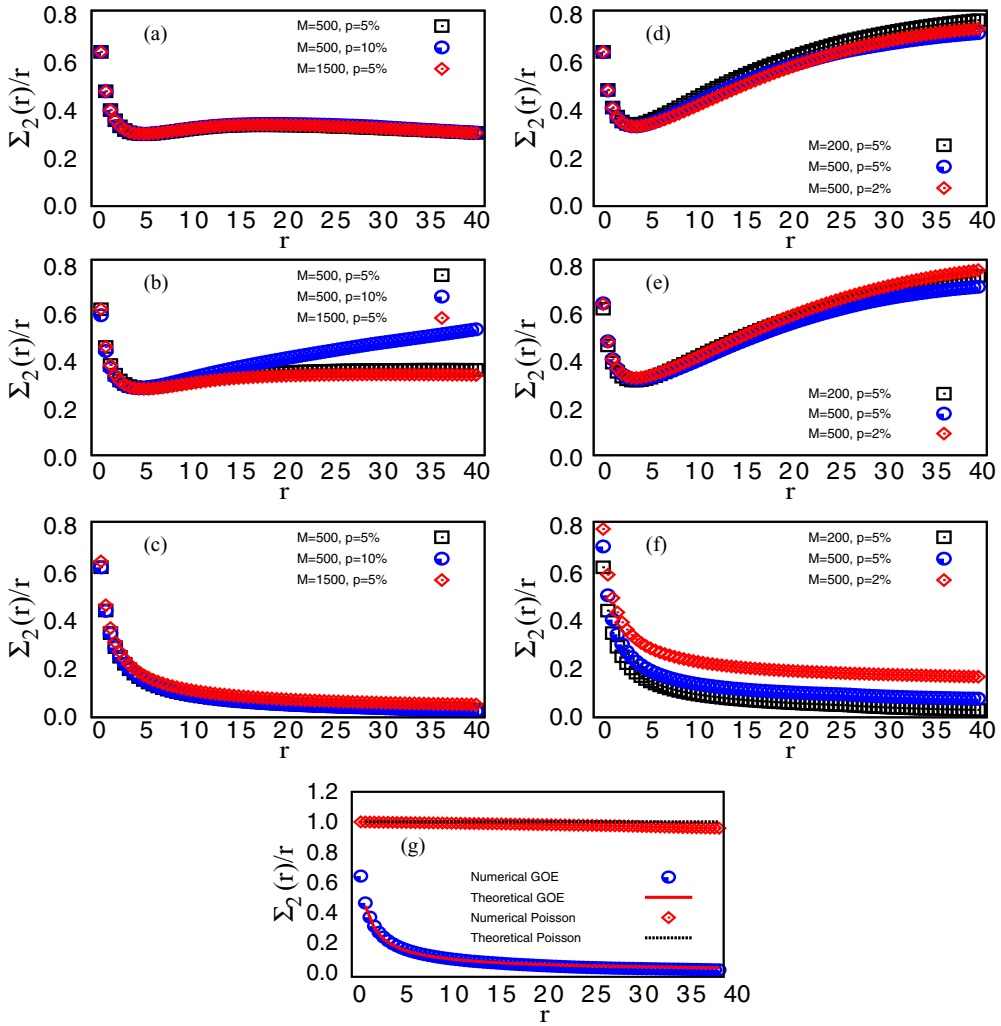

FIG. 4. Finite-size effect of the compressibility $\Sigma_2(r)/r$: The sensitivity of the number variance $\Sigma_2(r)$ to size N in a given energy regime is evident from Fig. 3. To probe it further, here we again consider the behavior for large N, namely, for $N = 10\,000$ (a–c) and $N = 25\,000$ (d–f) in three different energy regime [edge, (a) and (d); intermediate, (b) and (d); bulk, (c) and (f)]; the symbol "M" here refers to the ensemble size (number of matrices taken for one particular N) and the symbol "p" refers to the number of levels used for the numerics from the energy regime under consideration. As evident from the figures, the large-r behavior for $N = 25\,000$ approaches to a fractional compressibility (≈0.75 and 0.1, as expected from theoretical prediction [Eqs. (9) and (30)] in the intermediate and bulk regime, respectively). The behavior is, however, sensitive to "p" variation for a fixed "M," suggesting the nonstationarity of $\Sigma_2(r)$. As a consequence, it is not easy to implement the large-r limit necessary for the compressibility calculation. To validate the efficiency of our numerical code, a comparison of the numerically simulated result for GOE and Poisson ensemble with theory are shown in panel (g).

As mentioned in Sec. IV, the multifractal behavior of eigenfunction is described by a continuous set of scaling exponents τ_q [30]. The latter can be computed by standard box-size scaling approach. This is based on first dividing the system of L^d basis states into $N_l = (L/l)^d$ boxes (d is the dimension of the system and for our case, $d = 1$) and computing the box-probability μ_k of ψ in the ith box: $\mu_k(l) = \sum_n |\psi_n|^2$; here, $\sum_n$ is over basis-states within the kth box. This gives the scaling exponent τ_q for the typical average of $I_q(l) = \sum_{k=1}^{N_l} \mu_k^q(l)$:

$$\tau^{\rm typ}(q) = \frac{\langle \ln I_q(\lambda)\rangle}{\ln \lambda}, \tag{32}$$

where $\langle . \rangle$ is the average over many wave functions at the criticality. For numerical calculation of $\tau_q^{\rm typ}$, one usually considers the limit $\lambda \equiv l/L \to 0$, which can be achieved either by making $L \to \infty$ or $l \to 0$. We choose $\lambda = 0.1$ and carry out τ_q analysis for many N values, each considered for an ensemble size $M = 20$ (a large ensemble size M is not required for their analysis). For case $\mu = N$ and $q > 0$, the slope of τ_q versus q curve turns out to be $1/2$, which gives $D_q \approx 0.5$ [see Fig. 5(b)], which agrees well with our theoretical prediction [see Eq. (13)]. This is also confirmed in Fig. 5(c) displaying N-dependence of $\overline{\langle I_2\rangle}$, which is well-fitted by the expression $\overline{\langle I_2\rangle}(e_0\sqrt{N}, N) \approx 8e_0$. Rewriting in terms of e, this implies $\overline{\langle I_2\rangle}(e, N) \approx 8\frac{e}{\sqrt{N}}$ and, therefore, reconfirms $D_2 \approx 0.5$. Note, our result for D_q is in contrast with the study in Ref. [1], which theoretically predicts $D_2 \approx 2 - \gamma$ for $\mu \propto N^\gamma$ but numerically verifies the result only for the cases $\gamma \neq 1$.

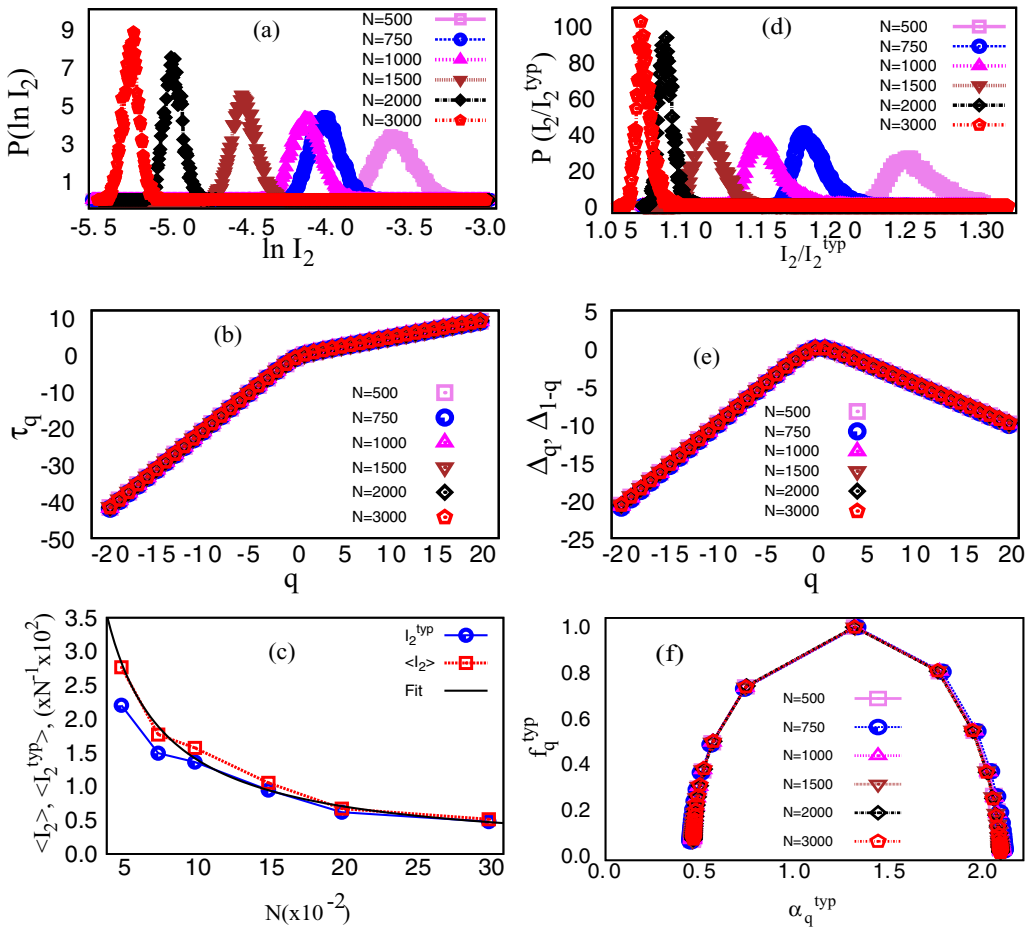

FIG. 5. Multifractality of eigenfunctions at intermediate regime: The figures display the distribution of IPR I_2 (spectral averaged locally) as well as multifractality spectrum for BE Eq. (28), with $\mu = N$, for many system sizes, at the intermediate energy regime: (a) $P(\ln I_2)$, distribution shifts along $\ln I_2$ axis preserving their form as N increases; (b) τ_q, as clear from the display, the straight line for $q > 0$ has a slope $\frac{d\tau_q}{dq} \approx \frac{1}{2}$, which agrees well with our theoretical prediction Eq. (13) (with $\gamma = 1$); (c) $\langle I_2\rangle(e_0\sqrt{N}, N)$ and $\langle I_2{}^{\rm typ}\rangle(e_0\sqrt{N}, N)$ (for clarity of presentation, here the rescaled variables $\frac{\langle I_2\rangle}{100N}$ and $\frac{\langle I_2{}^{\rm typ}\rangle}{100N}$ are displayed with respect to rescaled size $\frac{N}{100}$). The $\langle I_2\rangle$ curve fits well with $\frac{14.17}{N}$, which gives $D_2 \approx 0.5$ reconfirming our theoretical prediction (see discussion below Eq. (32) for clarification), (d) $P(I_2/I_2^{\rm typ})$, here the fit $f(I_2) = (\frac{I_2}{I_2^{\rm typ}})^{-1-x_2}$ at $I_2 \gg I_2^{\rm typ}$ gives $x_2 \gg 1$ (our numerics give $x_2 \approx 100$), which in turn implies $I_2^{\rm typ} = \langle I_2\rangle$; (e) anomalous dimension Δ_q, a symmetry around $q = 0$ is evident from the figure (see Sec. IV B), which also implies the symmetry of the singularity spectrum; (f) $f^{\rm typ}(\alpha_q)$, as suggested on theoretical grounds, $f^{\rm typ}(\alpha_q)$ [Eq. (33)] seems to approach a linear behavior in the region $\alpha < D_2 \approx 0.5$ and $\alpha > 1.5$ along with a parabolic behavior near $\alpha \sim 1$. The theory, however, predicts a narrowing parabolic regime as N increases.

Next, we numerically analyze the singularity spectrum using box-approach in which $f(\alpha)$ and α are defined as follows [39]: $\alpha_q^{\rm typ} = \lim_{\lambda\to 0} \frac{1}{\ln\lambda}\langle \frac{1}{I_q(\lambda)} \sum_{k=1}^{N_\lambda} \mu_k{}^q(\lambda)\ \ln\mu_k(\lambda)\rangle$ and

$$f\left(\alpha_q^{\rm typ}\right) = \lim_{\lambda\to 0}\frac{1}{\ln\lambda}\left[q\left\langle\frac{1}{I_q(\lambda)}\sum_{k=1}^{N_\lambda}\mu_k{}^q(\lambda)\ \ln\mu_k(\lambda)\right\rangle - \langle ln\ I_q(\lambda)\rangle\right], \tag{33}$$

with superscript "typ" on a variable implying its typical value. It is believed that the typical spectra is equal to the average spectra [i.e., $\tau_q^{\rm typ} = \tau_q$ and $f^{\rm typ}(\alpha) = f(\alpha)$] in the regime $q_- < q < q_+$ [30]. Here, $q_\pm$ corresponds to the values of q such that $f(\alpha_q) = 0$; the corresponding value of α_q are referred as $\alpha_\pm$, respectively. Our numerics of $f(\alpha)$ is confined within this regime. As displayed in Fig. 5(f) for six system sizes, $f(\alpha)$ behavior for the case $\mu = c_2 N$ is intermediate between the localized and delocalized limit. Also clear from the figure, α is contained in the interval (0,2), and $f(\alpha)$ satisfies the symmetry relation $f(2-\alpha) = f(\alpha) + 1 - \alpha$.

The symmetry $\Delta_q = \Delta_{1-q}$ in the spectrum of Δ_q can also be seen from Fig. 5(e). Our analysis gives $\alpha_0 = 1.3 > d, \alpha_1 = 0.74$, $f(\alpha_0) = d = 1$, $f(\alpha_1) = \alpha_1$. Above results are consistent with expected multifractal characteristics of the critical eigenstates [30,39].

The nonstationarity of the spectral statistics and existence of nonzero correlations between eigenfunctions and eigenvalues suggest the multifractality measures to be sensitive to chosen energy regime. This is also indicated by our theoretical analysis [see Eqs. (20) and (21)]; however, a local spectral averaging almost hides the energy dependence of $f(\alpha)$. The main reason

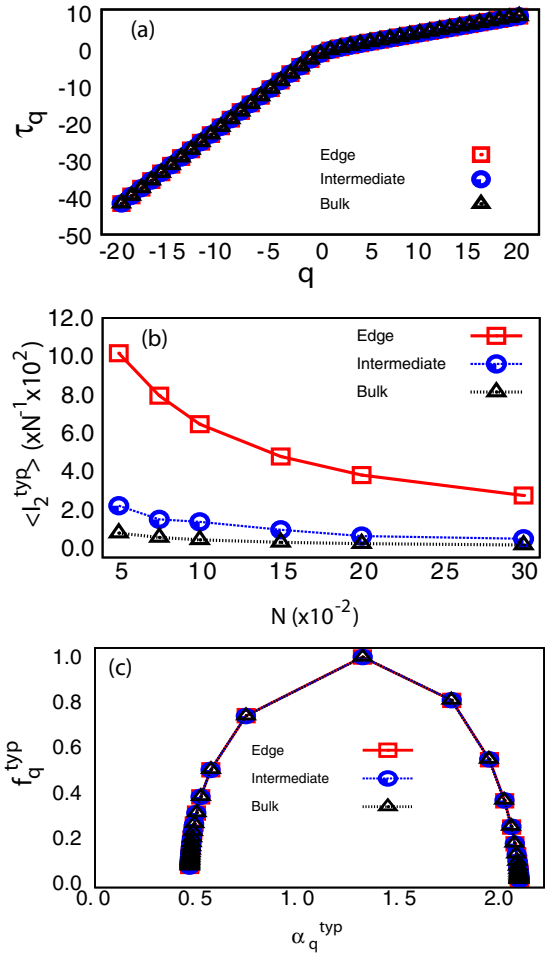

FIG. 6. Sensitivity of the multifractality to an energy regime: The figures display the multifractality spectrum for BE Eq. (28), with $\mu = N$ at three energy regimes. Although the energy dependence of $\langle I_2^{\rm typ}\rangle$ is clear from panel (b) but nearly same behavior of $\tau^{\rm typ}(q)$ in panel (a) [Eq. (32)] as well as $f_q(\alpha)$ behavior in panel (c) (both for $N = 3000$) for three energy ranges indicates a very weak sensitivity to energy range of these measures, which is further suppressed due to local spectral averaging.

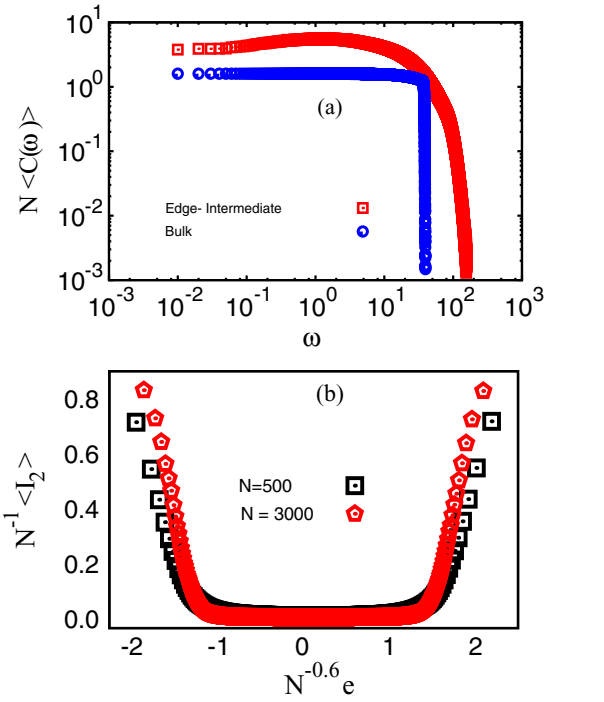

FIG. 7. Nonstationarity of two-point intensity correlation: The figures display the $\langle C(\omega)\rangle$ [Eq. (24), for $N = 3000$] and $\langle I_2\rangle$ (for $N = 500, 3000$) for BE Eq. (28), with $\mu = N$. In panel (a), the numerics is based on 20% levels in the energy range of interest. This leaves us only with two energy ranges for the analysis: "edge-intermediate" (as intermediate regime almost overlaps with edge) and "bulk." The function $N\langle C(\omega)\rangle \propto \omega$ for $\omega < 1$ and undergoes a power-law decay for $\omega > 1$; however, decay is faster than $1/\omega^2$ as predicted by theoretical calculation in Sec. IV C. As evident from panel (a), the decay rates are different in the two regimes, which is expected due to nonstationarity of $\overline{\langle I_2\rangle}$. As discussed in Sec. IV C, the energy-dependence of $\langle C\rangle$ comes from I_2, which varies rapidly for energy ranges away from bulk. This is verified in panel (b), which shows an almost constant $\overline{\langle I_2\rangle}$ in the bulk but a rapid increase around $e \sim N^{0.6}$ (note the figure shows the plot of $N^{-1}\ \overline{\langle I_2\rangle}$ with respect to rescaled $e \to e/N^{0.6}$). This confirms the sensitivity of $\langle C(e,\omega)\rangle$ to the energy regime of interest.

for this could be attributed to stronger sensitivity of the measures τ_q, $I_2^{\rm typ}$ to N-dependence. Figure 6 compares the ensemble averaged τ_q, $I_2^{\rm typ}$ as well as singularity spectrum for three different energy ranges; although the energy dependence of $I_2^{\rm typ}$ is clear from Fig. 6(b) but nearly the same behavior of τ_q, $f(\alpha)$ indicates an almost insensitivity of these measures to the energy scale. This is in contrast to spectral measures $P(s)$ and χ where the nonstationary effects are more pronounced.

To reveal the nonstationarity effects on the eigenfunction fluctuation, it is therefore necessary to consider a measure in which energy scales play an important role. As discussed in Sec. IV C, the two-point wave-function correlation is one such measure. Here we numerically analyze $\langle C(e,\omega)\rangle$, given by Eq. (24), for 20% energy levels chosen in bulk ($e \sim 0$) as well as in the intermediate-edge spectral regime. As discussed in Sec. IV C, the behavior of $\langle C\rangle$ is expected to change near $\omega \sim E_c$, with its curvature changing sign. Using the definition $E_c \sim \Delta_e\ N^{D_2}$, with $\Delta_e \propto N^{-1/2}$ and $D_2 = 0.5$, one has $E_c \sim 1$. As displayed in Fig. 7, the curvature of $\langle C\rangle$ curve indeed changes sign near $\omega \sim 1$, with $\langle C\rangle$ increasing for $\omega \leqslant 1$ and then undergoes a power law decay for $\omega > 1$. The decay, however, is faster than $1/r^2$ in both the regimes. As Λ_e in this case is size-independent, this is in agreement with theoretical prediction (see end of Sec. IV C). The figure also displays different decay rates in the two regimes which is expected due to different spectral rate of variation of $\overline{\langle I_2\rangle}$ in the bulk and intermediate; as can be seen from Fig. 8(b), $\overline{\langle I_2\rangle}$ is almost constant in the bulk but increases rapidly around $e \sim N^{0.6}$. This confirms the sensitivity of $\langle C(e,\omega)\rangle$ to the energy-regime of interest.

In the end, we compare our results for various critical measures with those in study [1]. For an ensemble density described by Eq. (28) with $\mu \propto N^\gamma$, the theoretical analysis of Ref. [1] predicts (i) $D_q = 2 - \gamma$ for $q > 1/2$, (ii) $f(\alpha) = \frac{\alpha}{2} + 1 - \frac{\gamma}{2}$ for $\alpha_{\rm min} < \alpha < \gamma$; here, $\alpha_{\rm min}$ depends on γ: $\alpha_{\rm min} = 0, 2-\gamma, \gamma$ for $\gamma > 2$ and $2 > \gamma > 1$ and $\gamma \leqslant 1$, respectively,

(iii) $K(\omega) \sim \frac{1}{\omega^2}$ for $\omega > E_c$ for all γ. Our theoretical analysis gives following results for the same ensemble: (i) $D_q = (2-\gamma)/2$ for spectrum bulk for $q > 1/2$, (ii) a linear $f(\alpha)$ for $\alpha < D_2$ and $\alpha \gg D_2$ but possibility of a parabolic behavior near $\alpha \sim 1$, (iii) $K(\omega) \sim \frac{1}{\omega^2}$ for $\omega > E_c$ only in bulk and for $1 < \gamma < 2$ (the latter corresponds to a size-dependent Λ_e with $N^{1-\gamma} < \Lambda_e \propto N^{2-\gamma}$). Λ_e being size-independent for $\gamma = 1,2$, the large ω-decay of $K(\omega)$ can be faster than $\frac{1}{\omega^2}$. Our theoretical predictions are corroborated by the numerical analysis of case $\gamma = 1$. (Note the study in Ref. [1] presents $K(\omega)$-numerics for $\gamma \neq 1,2$ only.) The deviation of our D_2-result from Ref. [1] may be due to their choice of a fixed size-dependence of the mean-level spacing ($\propto N^{-1}$) for all γ, while we have used $\Delta_e \propto N^{-\gamma/2}$; the latter result is derived in Ref. [34] and is confirmed by our numerics too (see Fig. 1).

VI. CONNECTION WITH OTHER ENSEMBLES

A Gaussian Brownian ensemble is a special case of a multiparametric Gaussian ensemble. As indicated by the studies [5,9,17], the eigenvalue distributions of a wide range of ensembles with single well potential, e.g., those with a multiparametric Gaussian measure and independent matrix elements, appear as a nonequilibrium stage of a Brownian-type diffusion process [17]. Here the eigenvalues evolve with respect to a single parameter, say Y, which is a function of the distribution parameters of the ensemble. The parameter is related to the complexity of the system represented by the ensemble and can therefore be termed as the spectral "complexity" parameter. The solution of the diffusion equation for a given value of the complexity parameter gives the distribution of the eigenvalues, and thereby their correlations, for the corresponding system. As the local spectral fluctuations are defined on the scale of local mean level spacing, their diffusion is governed by a competition between $Y - Y_0$ and local mean level spacing. Consequently, the evolution parameter Λ_e for the local spectral statistics is again given by Eq. (1) but with a more generic definition of Y (note so far the complexity parameter formulation has been analyzed in detail only in context of Gaussian ensembles although the studies in Refs. [13,17] indicate its validity for more generic cases). A single parameter formulation is also possible for the eigenfunction fluctuations but, contrary to spectral case, the parameter is not the same for all of them [14,17,28].

The implications of the complexity parametric formulation are significant: as the system dependence enters through a single parameter in a fluctuation measure, its behavior for different systems with the same value of the complexity parameter (although may be consisting of different combinations of the system parameters) will be analogous (valid for same global constraints; see Ref. [17] for details). An important point worth emphasizing here is the following: although the unfolding (rescaling by local spectral density) of the eigenvalues removes their dependence on the local spectral scale, the latter is still contained in Λ_e. The spectral dependence of Λ_e varies from system to system. Thus, two systems in general may have the same spectral statistics at a given spectrum point, but the analogy need not extend for a spectral range of sufficient width. It could, however, happen in a case where the two systems have the same local rate of change of Λ_e along the spectrum, which usually requires a similar behavior for the local spectral density. The analogy implied by the complexity parameter formulation is, therefore, strictly valid only in the case of the ensemble averaging. It can, however, be extended to include spectral averaging within the range in which the local density is almost stationary.

The AE consisting of Anderson Hamiltonians, the PRBM ensemble, and the Brownian ensemble appearing during Poisson → GOE transition belong to same global symmetry class (time-reversal symmetry preserved). Based on the complexity parameter formulation, therefore, the critical point statistics of an AE or PRBME can be mapped to that of the Poisson → GOE Brownian ensemble. The validity of the mapping was indeed confirmed by a number of numerical studies [5,23]. As discussed in Refs. [5,23,28], the critical BE analog of a critical AE is unique; similar to an AE, the level-statistics of the BE shows a scaling behavior too. The study in Ref. [1], however, claims that the critical point behavior for an Anderson ensemble and a PRBM ensemble differ from that of a Rosenzweig-Porter ensemble (same as the Brownian ensemble between Poisson → GOE cross-over). For example, the study shows that the correlation $C(\omega)$ between two wave functions, at energies e and $e+\omega$, decays as $\omega^{-\mu}$ for $\omega \gg E_{\rm th}$, with $\mu = 2$ for Rosenzweig-Porter ensemble and $\mu = D_2 - 1$ for Anderson Hamiltonian and PRBM ensemble. Here, $E_{\rm th} \sim N^{-z}$ is the Thouless energy (same as E_c used in context of BEs), with $z = 1$ for AE and PRBME and $z < 1$ for the BE. These results are, however, based on the assumption of local stationarity of the spectral density around which the fluctuations are measured. The seeming contradiction of the results between Refs. [1] and [5] originates in the range of validity of the assumption. As indicated by previous studies, the ensemble averaged bulk spectral density of an Anderson ensemble is almost similar in behavior as that of a PRBM ensemble but is different from that of the Poisson → GOE Brownian ensemble. In the latter case, it varies more rapidly along the spectrum (see Sec. V); the spectral range r of local stationarity in the case of the BE is, therefore, much smaller than the AE and PRBME, and the measures (e.g., compressibility), which are based on large r-limit considerations, may not be appropriate for the comparison. Indeed, the complexity parameter-based formulation permits a comparison of the measures for each spectral point and is, therefore, more suitable for a comparative analysis of cases with different spectral densities.

VII. CONCLUSION

Based on a nonperturbative diffusion route, we find that the criticality of the fluctuation measures for the BEs is sensitive to both spectral scale as well as the perturbation strength. Our theoretical results are applicable for both Gaussian as well as Wishart BEs of the Hermitian matrices, with or without time-reversal symmetry and appearing during transition from an arbitrary initial condition to stationary ensembles. The results are confirmed by a numerical analysis of the BEs appearing during Poisson to GOE transition. The relevance of our BE-results is expected to be wide-ranging. For example, BEs are connected to the ensembles of column constrained matrices and the latter has applications in many area, as discussed in Ref. [18]. Further, using the complexity

parameter-based mapping of the fluctuation measures of a BE to a multiparametric Gaussian ensemble [17], the results derived here are useful for the latter too.

An important outcome of our analysis is to reveal a new criteria for the criticality of the random matrix ensembles, i.e., the spectral complexity parameter. The latter has been shown to govern the evolution of all spectral fluctuation measures for a multiparametric ensemble including BEs [17]; the search for criticality, therefore, need not depend on a specific measure, e.g., compressibility. Using the complexity parameter, it is easier to find the number of critical points too: the spectral statistics has a critical point at a fixed energy if the size-dependence of the perturbation strength Y is the same as that of the square of the mean level spacing. The appearance of two critical points in the case of the BE between Poisson and GOE (i.e., the Rosenzweig-Porter ensemble) can, therefore, be attributed to the variation of the level density from a Gaussian to semicircle form. This also predicts the existence of two critical points in a Wishart Brownian ensemble, which appears during Poisson to WOE transition; this follows because their level density changes from exponential decay to the $\sqrt{a-e}$ form (with a as a constant; see discussion below Eq. (21) of Ref. [14]). The existence of two critical points was recently reported in the context of other complex systems too, e.g., many-body localization as well as random graphs [33].

The complexity parameter has another advantage over previous measures for criticality, which were often based on the assumption of the local ergodicity. As the search for the criticality originated in context of disordered systems, usually with large flat regions in the bulk level density, the local ergodicity considerations were easily satisfied. In general, however, this is not the case, e.g., for systems with rapidly changing level densities. The measures based on the ensemble averaging only, or those based on averaging over very small spectral ranges, are more appropriate choices to seek critical point in such cases.

The present work deals with the BEs taken from Hermitian matrix space. An understanding of critical BEs lying between the pairs of stationary ensemble subjected to other global constraints, e.g., non-Hermiticity (e.g., circular ensembles), chirality, and column constraints still remains an open question.

[1] V. E. Kravtsov, I. M. Khaymovich, E. Cuevas, and M. Amini, New J. Phys. **17**, 122002 (2015).
[2] P. Shukla, New J. Phys. (IOP) **18**, 021004 (2016).
[3] C. L. Bertrand and A. M. Garcia-Garcia, Phys. Rev. B **94**, 144201 (2016).
[4] N. Rosenzweig and C. E. Porter, Phys. Rev. **120**, 1698 (1960).
[5] P. Shukla, J. Phys.: Condens. Matter **17**, 1653 (2005); Phys. Rev. E **62**, 2098 (2000).
[6] F. Dyson, J. Math. Phys. **3**, 1191 (1962).
[7] M. L. Mehta, *Random Matrices* (Academic Press, San Diego, 1991).
[8] A. Pandey, Chaos Solitons Fractals **5**, 1275 (1995).
[9] P. Shukla, Int. J. Mod. Phys. B (WSPC) **26**, 1230008 (2012).
[10] A. Pandey and P. Shukla, J. Phys. A **24**, 3907 (1991).
[11] S. Kumar and A. Pandey, Ann. Phys. **326**, 1877 (2011).
[12] Vinayak and A. Pandey, Phys. Rev. E **81**, 036202 (2010).
[13] P. Shukla, Phys. Rev. Lett. **87**, 194102 (2001).
[14] P. Shukla, arXiv:1609.07290.
[15] A. Altland, M. Janssen, and B. Shapiro, Phys. Rev. E **56**, 1471 (1997).
[16] M. Janssen, Phys. Rep. **295**, 1 (1998).
[17] P. Shukla, J. Phys. A **41**, 304023 (2008); Phys. Rev. E **71**, 026226 (2005).
[18] P. Shukla and S. Sadhukhan, J. Phys. A **48**, 415003 (2015); **48**, 415002 (2015).
[19] B. I. Shklovskii, B. Shapiro, B. R. Sears, P. Lambrianides, and H. B. Shore, Phys. Rev. B **47**, 11487 (1993).
[20] J. T. Chalker, V. E. Kravtsov, and I. V. Lerner, Pis'ma Zh. Eksp. Teor. Fiz. **64**, 355 (1996) [JETP Lett. **64**, 386 (1996)].
[21] B. L. Altshuler, I. Kh. Zharekeshev, S. A. Kotochigova, and B. I. Shklovskii, Zh. Eksp. Teor. Fiz. **94**, 343 (1988) [Sov. Phys.-JETP **67**, 625 (1988)].
[22] A. D. Mirlin, Y. V. Fyodorov, F.-M. Dittes, J. Quezada, and T. H. Seligman, Phys. Rev. E **54**, 3221 (1996).
[23] R. Dutta and P. Shukla, Phys. Rev. E **76**, 051124 (2007).
[24] J. B. French, V. K. B. Kota, A. Pandey, and S. Tomsovic, Ann. Phys. (NY) **181**, 198 (1988).
[25] K. M. Frahm, T. Guhr, and A. Muller-Groeling, Ann. Phys. (NY) **270**, 292 (1998).
[26] F. Leyvraz and T. H. Seligman, J. Phys. A **23**, 1555 (1990).
[27] H. Kunz and B. Shapiro, Phys. Rev. E **58**, 400 (1998).
[28] P. Shukla, Phys. Rev. E **75**, 051113 (2007).
[29] J. M. G. Gómez, R. A. Molina, A. Relaño, and J. Retamosa, Phys. Rev. E **66**, 036209 (2002); O. Bohigas and M. J. Giannoni, Ann. Phys. **89**, 422 (1975); I. O. Morales, E. Landa, P. Stransky, and A. Frank, Phys. Rev. E **84**, 016203 (2011).
[30] F. Evers and A. D. Mirlin, Rev. Mod. Phys. **80**, 1355 (2008).
[31] R. Bhatt and S. Johri, Int. J. Mod. Phys. Conf. Ser. **11**, 79 (2012).
[32] J. T. Chalker, Physica A (Amsterdam) **167**, 253 (1990); J. T. Chalker and G. J. Daniell, Phys. Rev. Lett. **61**, 593 (1988).
[33] E. Cuevas and V. E. Kravtsov, Phys. Rev. B **76**, 235119 (2007).
[34] M. Kreynin and B. Shapiro, Phys. Rev. Lett. **74**, 4122 (1995); B. Shapiro, Int. J. Mod. Phys. B **10**, 3539 (1996).
[35] J.-L. Pichard and B. Shapiro, J. Phys. I (France) **4**, 623 (1994).
[36] S. Tomsovic, Ph.D Thesis, University of Rochester (1986); G. Lenz and F. Haake, Phys. Rev. Lett. **67**, 1 (1991); V. K. B. Kota and S. Sumedha, Phys. Rev. E **60**, 3405 (1999).
[37] O. Bohigas and M. J. Giannoni, Ann. Phys. **89**, 393 (1975).
[38] M. V. Berry and P. Shukla, J. Phys. A **42**, 485102 (2009).
[39] A. Rodriguez, L. J. Vasquez, and R. A. Romer, Eur. Phys. J. B **67**, 77 (2009).